C.S.O. COSTRUZIONE STRUMENTI OFTALMICI

ATLAS OF ANTERIOR SEGMENT OCT

CONTRIBUTORS

Giovanni Alessio, Jorge L. Alió del Barrio, Andrea Bedei, Antonio Calossi, Francesco Carones, Marco Fantozzi, Gian Luca Laffi, Claudio Macaluso, Leonardo Mastropasqua, Rita Mencucci, Antonio Moreno, Giacomo Savini, Domenico Schiano Lomoriello

FABIANO EDITORE

C.S.O. COSTRUZIONE STRUMENTI OFTALMICI

ATLAS OF ANTERIOR SEGMENT OCT

CONTRIBUTORS

Giovanni Alessio, Jorge L. Alió del Barrio, Andrea Bedei, Antonio Calossi, Francesco Carones, Marco Fantozzi, Gian Luca Laffi, Claudio Macaluso, Leonardo Mastropasqua, Rita Mencucci, Antonio Moreno, Giacomo Savini, Domenico Schiano Lomoriello

FABIANO EDITORE

Publisher:
FGE S.r.l.
Fabiano Gruppo Editoriale
Field office: Regione Rivelle 7/F - 14050 Moasca AT, Italy
Editorial office: Via Petitti 16, 20149 Milano, Italy
e-mail: info@fgeditore.it - Tel. +39 0141 1706694

Editorial coordination: Vittorio Picardo M.D.

Graphics: Viola Mura

Translator: Michela Cimberle - Eugenio Albert

Printing: FGE S.r.l.

Some images come out from doctors records in different languages.

This publication was made possible due to the essential contribution of:

C.S.O. S.R.L. COSTRUZIONE STRUMENTI OFTALMICI
Via degli Stagnacci 12/E
50018 Scandicci - Florence, Italy
http://www.csoitalia.it/

ISBN: 978-88-97929-87-1

Printed in: September 2018

C.S.O. COSTRUZIONE STRUMENTI OFTALMICI

ATLAS OF ANTERIOR SEGMENT OCT

CONTRIBUTORS

Giovanni Alessio, Jorge L. Alió del Barrio, Andrea Bedei, Antonio Calossi, Francesco Carones, Marco Fantozzi, Gian Luca Laffi, Claudio Macaluso, Leonardo Mastropasqua, Rita Mencucci, Antonio Moreno, Giacomo Savini, Domenico Schiano Lomoriello

FABIANO EDITORE

INDEX AS-OCT ATLAS

INTRODUCTION

The evaluation of corneal and anterior segment morphology and structure has been recently improved thanks to several diagnostic instruments, which allow us to obtain even more detailed and precise information.
In my thirty year-long career, I have had the pleasure of being part of the birth, the growth and the global diffusion of several diagnostic technologies that, today, are part of our routine armamentarium for the anterior segment analysis.

Since my graduation as a medical doctor in 1988, I have witnessed the entire process starting from idealization to commercialization of videokeratography for the measurement of the anterior corneal curvature.

I experienced the advent of the first Scheimpflug cameras for the visualization of the anterior chamber and the evaluation of the posterior corneal curvature.

I saw great ideas arise and then fall (corneal holography, raster-stereography), other ones taking off but never becoming widely spread (high-frequency ultrasonography) either due to the high associated costs, or from difficult to understand strategical and commercial decisions. I have also observed techniques for the anterior segment developed and applied to the posterior segment, such as optical coherence tomography (OCT).

This Atlas celebrates the introduction of a combined diagnostic technology that allows to obtain very high-resolution images, and consequently extremely accurate and precise anatomy-topographical data, related to several structures of the anterior segment: tear film, corneal epithelium, Bowman membrane, corneal stroma, corneal endothelium, anterior and posterior corneal curvature, anterior chamber, iris-sclera-corneal angle, iris, pupil size and dynamics, crystalline lens.

All of this is possible due to the combination of the highest technology for the analysis of the anterior corneal curvature (videokeratography Placido-disc based), with quality spectral domain OCT, found in a single instrument that has yet many other innovative technical features. In the time of a "click", this instrument provides a complete, yet detailed panorama of the anterior segment.

In other words, this is the coupling of the best corneal topographer and the best anterior segment OCT, with a commercial name, MS-39, that recalls the founder of the company, the father of this technology. This system is perfectly integrated with the CSO diagnostic platform (aberrometer, Scheimpflug camera, corneal topographer, etc.) which connects in an interactive way to provide even more diagnostic information.

I had the opportunity to use one of the first MS-39 prototypes in my clinical practice. After almost one year of daily use, I can honestly say that I could no longer practice without it. If I had to choose one single diagnostic tool to work with, no doubt, this one would be my choice. As a corneal, refractive and cataract surgeon I have to admit I learned so much from the information, previously unknown, provided by this technology.

There are countless clinical examples, most of them illustrated in this Atlas, that helped me find an easier diagnostic/surgical direction only through the use of this instrument. And it has been so wonderfully exciting, over my thirty years of ophthalmology practice, to witness the path CSO has made side by side with the ophthalmologists. Indeed, for ophthalmology, CSO was already there thirty years ago when, beside slit lamps and keratometers, its innovation was demonstrated by the launch of one of the very first videokeratographers.

Today CSO is present with this one-of-a-kind technology and it is destined to force all the competitors to strive to keep up with this shining example of the Italian excellence. For all these reasons, I strongly wish that CSO achieves all the popularity that it deserves for the innovation and development of this diagnostic technology. Empowered by this technology, future achievements of the scientific community will arise by enabling research thanks to an instrument capable to evaluate, measure and visualize information that was not accessible before. These advances will make our profession easier and more efficient, allowing us to provide our patients, the final consumers, with continuously better and more efficient services.

Milan, September 2018

Francesco Carones

SPECIAL SECTION

TECHNOLOGY AND INTERPRETATION

CSO MS-39: A NEW ANTERIOR SEGMENT OCT COMBINED WITH PLACIDO DISC TOPOGRAPHY

Gabriele Vestri[1], M.S.E.* - Claudio Macaluso[2,3], M.D. - Lorenzo Rosellini[1], M.S.E.* - Stefano Faini[1], M.S.E.*
Francesco Versaci[1], M.S.E.* - Simone Spadini[1], B.S.C.** - Matteo Marcacci[1] - Juri Ceccherelli[1] - Simone Donati[1], B.S.C.**
[1] CSO Costruzione Strumenti Oftalmici, Florence, Italy
[2] University of Parma, Parma, Italy
[3] IMEM-CNR (National Research Council), Parma, Italy
* M.S.E.: Master Science in Engineering
** B.S.C.: Bachelor in Science

INTRODUCTION

Over the last three decades, there has been a constant evolution of diagnostic instrumentation for the anterior ocular segment imaging. The first instruments used were corneal topographers, based either on reflection or projection of a known pattern of mires, which allowed an accurate automated measurement in one single aquisition of a large area of the anterior corneal surface. Corneal topographers have provided the clinician with the possibility to easily detect mild keratoconus and irregular astigmatism, to measure the corneal contribution to ocular aberrations, and in general, to better understand the anterior corneal surface from a geometrical and optical point of view.

The second generation devices were optical scanning instruments, which enabled the capture of image sections of the whole anterior segment, thus adding visual and quantitative information about the posterior corneal surface and the anterior chamber (iris, angles and anterior surface of the crystalline lens). The first of these instruments was the Orbscan (Bausch & Lomb, Rochester, NY), that was based upon anterior segment scanning through a translating illuminating slit combined with an observation system. This was then followed by a series of instruments, such as Pentacam (Oculus Optikgeräte, Wetzlar, Germany), Galilei (Ziemer, Swizerland), Sirius (CSO, Florence, Italy) and TMS4 (Tomey, Japan) that are based upon a rotational scanning slit utilizing Scheimpflug principle, which allows to tilt the axis of the observation system while maintaining in focus the whole plane of the illuminated section.

With these advancements, clinicians were able to obtain new information regarding their patients, such as elevation maps of the anterior and posterior corneal surface and pachymetry maps to detect keratoconus and ectasia. They were also able to measure posterior and total corneal astigmatism to calculate the power of toric intraocular lenses (IOLs). Finally, they were able to assess the total corneal power by ray-tracing to calculate IOL power after corneal refractive surgery. Scheimpflug imaging, however, had limitations, related to the low resolution and poor quality of anterior segment scans and the presence of artifacts when tissue scattering is excessive.

The third generation was the application of OCT technology to produce better images with higher definition. The first OCT instrument fully dedicated to the anterior segment was the Visante (Carl Zeiss Meditec, Dublin, CA). In comparison with retinal OCTs, further refinement of the anterior segment technology were progressing relatively slow. Some limitations of the Visante were:

- the slow scanning speed and consequently low number of acquired sections;
- the limited reliability of measurements, which made it necessary to combine the corneal topographer Atlas (Carl Zeiss Meditec AG, Jena, Germany) for the measurements of the anterior corneal surface;
- the lower image quality as compared with retinal OCTs with corneal adaptor modules.

Later advancements were developed with retinal OCT technology, equipped with corneal adaptor modules. Further developments gave origin to the first instruments dedicated exclusively to the anterior segment, including the Casia SS-1000, followed by the Casia 2 (Tomey, Nagoya, Japan) and recently by the MS-39 (CSO, Florence, Italy). These devices allow the acquisition of high quality anterior segment angle-to-angle images as well as high-speed scanning of a large number of meridians for accurate topographic corneal maps.

OCT SYSTEMS – BASIC CONCEPTS

Until recently, OCT has been used mainly for the retina, with limited applications to the measurement of anterior segment structures, namely the axial length. Manufacturers are only now directing their attention to new OCT systems able to provide topographic and tomographic analysis of the cornea. This delay has been mainly due to the complexity and consequently high costs of this technology. Reliability was also an issue, since the old generation OCT systems were unable to provide images of the entire anterior segment and to acquire accurate measurements, comparable or better than those provided by less sophisticated technologies.

OCT is a technology based upon the measurement of the interference of two beams of a broadband radiation (typically infrared) from a reference arm and a sample arm[1-4].

To put it simply, the radiation emitted from a broadband source - usually an infrared super-luminescent diode (SLD) - is in part transmitted to a reference arm and in part to a sample arm. A mirror, placed at the end of the reference arm, reflects the beam back towards a fourth arm (detection arm) on which a photo-detector is placed. Similarly, the radiation sent to sample arm is backscattered by the ocular tissues towards the detection arm, where it interferes with the return beam from the reference arm. If the reference mirror is moved, thereby altering the length of the reference arm, the interference of the ocular structures encountered by the incident beam of the sample arm can be sampled at various depths. In practice, the photodiode reveals a peak signal for each backscattering element encountered by the beam incident on the sample at a position corresponding to that of the movable mirror of the reference arm. This pattern is found in Time Domain OCT (TD-OCT) and is shown in Figure 1a. It was first applied in the field of ophthalmology for the measurement of the inter-distances between the various ocular structures, in particular the axial length of the eye, the corneal thickness, the anterior chamber depth and the thickness of the crystalline lens. With this technique, moving the reference mirror is necessary to obtain a response from the structures at various depths. A velocity limit occurs when it is necessary to make a scan of several contiguous lines (A-scan) in order to create an image of an ocular section (B-scan). Eye movements during a slow scan lead to an unwanted and uncorrectable distortion of the image.

A more complex implementation, known as Fourier Domain OCT (FD-OCT), eliminates the need for a moving reference mirror to obtain measurements at various depths. This allows high-speed acquisition of axial scans that reduce artifacts due to eye movements. The Fourier Domain OCT, in addition to decreasing the time of acquisition, also presents advantages in terms of signal-to-noise ratio compared to the Time Domain. The basic concept is to measure the spectral interference between the radiation returning from the reference arm and the sample arm in a certain range of wavelengths emitted by the source. This means that, in a single A-scan, for each wavelength that the detection arm collects, the interference value of the returned radiation is determined by the sample and reference arms.

The set of these values at various wavelengths is processed with more or less complex algorithms, basically containing a Fourier transformation, to obtain the reflectivity profile of the sample along an axis.

The Fourier Domain OCT devices can be in turn classified into the following two classes depending on how they acquire the interference values at various wavelengths: Spectral Domain OCT (SD-OCT in Figure 1b) and Swept Source OCT (SS- OCT in Figure 1c).

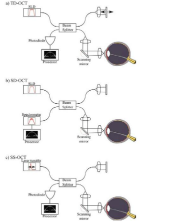

Figure 1. *OCT setups: a) Time domain b) Spectral Domain and c) Swept Source.*

The first class of these instruments uses a broadband source that emits a certain range of wavelengths all at the same time. The detection arm contains a spectrometer to decompose the interference signal deriving from the returned radiation of the sample and reference arms into its components of the various wavelengths. Therefore, in a single acquisition, the sensor of the spectrometer collects the spectrum necessary to determine the reflectivity profile along an axis of the sample.

The second class of devices uses a light source that is a tunable laser, i.e. a laser whose wavelength can be varied very rapidly[6]. The light source is driven to emit the various wavelengths in sequence and is synchronized with a photodiode, which replaces the spectrometer on the detection arm. A processing unit associates the wavelengths emitted by the source to the values measured by the photodiode, and reconstructs the interference spectrum between the beams coming back from the reference and sample arms.

TECHNICAL FEATURES OF MS-39

OCT SUBSYSTEM

The MS-39 contains an SD-OCT system with a broadband light source emitting a radiation centered around 850 nm. The spectrometer inside the instrument collects an interval of wavelengths of approximately 80 nm thus ensuring an axial resolution of 4.8 µm in air (about 3.5 µm in tissue) and an imaging depth of about 10 mm in air. The scanning subsystem is based on two galvanometric mirrors, which deviate the beam according to the numeric preset or configurable trajectories and it allows a maximum transversal field of 16 mm and a transversal resolution of 35 µm.

There are two basic reasons why the SD-OCT technology was chosen instead of the SS-OCT for the MS-39. First, although the SS-OCT exhibits some undeniable advantages like a higher scan rate and a greater imaging depth, the SD-OCT technology allows for an axial resolution that is twice that of the best SS-OCT systems (5 µm as compared with 10 µm). Second, the SD-OCT is considerably less expensive.

To the best of our current knowledge, the axial resolution of the MS-39 is the highest of all OCT instruments available on the market today, for both the anterior segment and the retina. It must be emphasized that this feature is extremely important for the resolution of the details in the corneal strata, in particular for the epithelium. The imaging depth of the MS-39 is the highest of all the ophthalmic SD-OCT instruments on the market.

The shorter wavelength was chosen to favor the image detail in the corneal layers rather than a better penetration into the tissue by longer wavelengths. The latter, on the other hand, has the advantage of imaging deeper structures such as the scleral spur or the posterior surface of the iris.

INTEGRATION WITH PLACIDO DISC TOPOGRAPHY

Why was it necessary to equip with Placido disc Topography an advanced OCT system like the MS-39, characterized by high axial resolution (5 µm in air) and capable of imaging the edge of the anterior corneal surface? The answer can be found through quantitative analysis of the accuracy necessary to get a reliable measurement of the anterior corneal curvature. To illustrate this point, let's compare the height profile of two spheres with curvatures of 42.75 D and 43.00 D (7.89 and 7.85 mm), i.e. with a difference of curvature of 0.25 D. The height difference between two meridional sections of the two spheres is about 0.4 µm at 1 mm from the center and 1.5 µm at 2 mm (Figure 3). If these values are compared with the axial resolution of the OCT system in air and if we consider that one of the primary purposes of the instrument is the accurate measurement of corneal surfaces, the need to add a system with a greater sensitivity like the Placido disc becomes evident.

In MS-39 software, for all cases where keratoscopy is available and reliable (i.e. the anterior

Figure 2. CSO Srl, MS-39

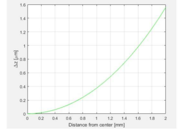

***Figure 3.** Difference in the height profile of two spheres with curvatures of 42.75 D and 43 D (7.89 and 7.85 mm)*

corneal surface is not very irregular or damaged), the measurement of the anterior surface obtained by Placido disc is preferred to the measurement done with the OCT subsystem.

ACQUISITION

The MS-39 offers the clinician a wide range of diagnostic options thanks to the different available acquisition modes.

TOPOGRAPHY

Topography is the acquisition mode for collecting the images necessary for the measurement of the anterior segment of the eye, i.e. for the generation of the classical curvature, power, and height maps of the corneal surfaces and of anterior chamber depth.

Three options are available for the OCT star scanning pattern of meridional sections at equally spaced angular positions:

1) 25 B-scans, each made up of 1024 A-scans, of 16 mm sections captured in a time lapse of about 1 second (Figure 4a).
2) 12 B-scans over a width of 16 mm, each made up of 1024 A-scans and resulting from the average of the 2 images of the same meridian, captured in a time lapse of about 1 second.
3) 12 B-scans over a width of 10 mm, each made up of 600 A-scans and resulting from the average of the 5 images of the same meridian, captured in a time lapse of about 1.5 seconds.

The second and third options can be used to produce higher quality images over the full transverse field or a reduced central portion of it.

During the OCT scan, two frontal images of the eye, one for keratoscopy and the other for the iris, are also captured with a field of view of about 14.1 x 10.6 mm.

SECTION

IMAGES

This is a very important acquisition mode, which recalls the use of the slit lamp, but with

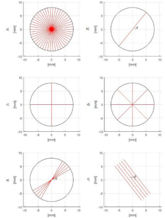

Figure 4. Scanning patterns: a) Star scanning for topography (25 sections), b) Line scanning, c) Horizontal and vertical lines (2x), d) Four meridians (4x), e) Sector scanning with 5 lines, f) Raster scanning with 5 lines and inter-distance equal to 1 mm

the fundamental difference that the captured images can be used for accurate measurements.

There are two image quality options:

- High definition: several images of the same section are captured in order to calculate an average image in which the presence of the speckle is drastically reduced
- Raw image: this option is faster than the previous one as there is no averaging of multiple captures; it is useful when the patient is not very cooperative in order to speed up the acquisition time

The sectional images can be acquired at various orientations (Figure 4b) by selecting the angle through a rotating wheel on the top of the joystick or by clicking the direction on the en face corneal image.

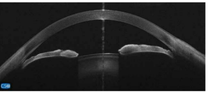

***Figure 5.** A typical anterior segment OCT scan as performed by MS-39. High definition imaging of the anterior ocular structures is possible. The corneal epithelial layer is perfectly delineated, as shown by the transition from cornea to conjunctiva in the limbal region. Details of the normal structure of the stroma, including minimal changes of transparency approaching the limbal area, can be fully appreciated due to the 850 nm wavelength of the instrument, which is close to the wavelength of visible light. The iridocorneal angle and the iris stroma, including the posterior pigmented epithelium, as well as the crystalline lens within the pupillary aperture, can be visualized in fine detail. Unfortunately, no OCT can penetrate the eye beyond the iris pigmented epithelium, even those utilizing longer wavelengths, leaving the investigation of other ocular structures (e.g. ciliary body tumors) to other more invasive means, including ultrasounds, CT and MRI.*

The width of the transversal field of view can be chosen by the user with the 10 or 16 mm options, respectively dedicated to the analysis of details in the layers of a limited corneal section and for an overall view of the anterior segment. In order to determine pupil dilation status, three illuminating conditions are available during the acquisition: scotopic, mesopic and photopic. In order to optimize the daily workflow of a clinical practice, some preset scanning patterns are made available:

- 2x: two sections at 90° degrees are acquired, one in the horizontal and one in the vertical direction (Figure 4c)
- 4x: four sections are acquired at equi-spaced angular orientations, one at 0°, one at 45°, one at 90° and one at 135°(Figure 4d)
- Sector: within a sector, the orientation and angular amplitude of which can be chosen by the user, an odd number from 3 to 7 sections can be captured at equi-spaced angles (Figure 4e)
- Raster: an odd number from 3 to 7 sections are captured at an orientation and interline distance chosen by the user. The interline distance can be adjusted from 0.3 to 1 mm (Figure 4f).

VIDEO

The video acquisition mode is useful when the user is interested in observing a non-stationary phenomenon. It can be helpful in analyzing the iris motion, the possible closure of the iridocorneal angle (dynamic gonioscopy) and the ICL vaulting changes at different luminous conditions, or to document the presence of floating elements in the aqueous (e.g. fibrins after cataract surgery).

LENS BIOMETRY

This acquisition mode is available to measure the lens thickness and to estimate the position of the equatorial plane of the lens. In this case, two sections, one horizontal and the other vertical, are acquired over a width of 16 mm.

PUPILLOGRAPHY

The MS-39 offers a specific examination for

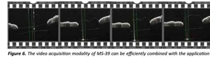

Figure 6. The video acquisition modality of MS-39 can be efficiently combined with the application of standardized luminance conditions obtained by controlling the Placido disc. Besides observing both angular morphology and pupil dynamics that occur with changes in illumination, a fine fibrin membrane occluding the whole pupillary area the first day following cataract surgery can be visualized, and its movements observed while it is protruding into the anterior chamber when pupillary constriction is elicited by light.

the measurement of the pupil position and diameter in several light conditions: scotopic, mesopic, photopic and dynamic, i.e. during the transition from a high photopic condition to a scotopic one. This exam is often underestimated or completely neglected in the clinical practice, but it is very important, in general, for the assessment of the optical quality of the anterior segment of the eye. Specific applications can be accomplished, such as the pre-operative evaluation of a candidate for refractive surgery, the decision on whether to implant a multifocal IOL or the post-operative evaluation of the optical zone of a patient who has undergone refractive surgery.

MAPS

As an evolution of the CSO Sirius topographer-tomographer, the MS-39 is able to measure all the classical maps of the anterior segment of the eye (Figure 7):

- Sagittal and local curvature maps of both the anterior and posterior corneal surfaces
- Altimetric maps of both the anterior and posterior corneal surfaces
- Refractive power maps for both the corneal surfaces and for the entire cornea
- Corneal thickness
- Anterior chamber depths
- Gaussian curvature for the anterior corneal surface
- Wavefront error maps for the entire cornea and for the anterior and posterior corneal surfaces alone

By exploiting its superior imaging capability in resolving corneal layers, the MS-39 is also able to calculate the epithelial and stromal thickness maps over an 8 mm diameter.

CORNEAL EPITHELIUM AND STROMAL MAPS

The corneal epithelium is the most anterior corneal surface which protects the eye and also plays an important role in maintaining a high optical quality. The epithelium is not homogeneous in thickness and compensates for possible stromal surface irregularities, becoming thicker over valleys and thinner over hills where the stroma protrudes. In general, it tends to regularize abrupt changes in stromal thickness[7].

As a consequence, the front corneal surface may appear smoother on topography than the underlying anterior stroma. Therefore, corneal analysis based on topography and pachymetry with no knowledge of epithelial thickness may be misleading and result in an incorrect assessment of pre-operative keratoconus[8] and post-refractive surgical ectasia progression.

During recent years corneal epithelium assessment has become a hot topic. Numerous reports have been published describing central epithelial thickening following myopic excimer laser ablations[9-19], which has been related to myopic regression. Epithelial thickness changes have also been described after orthokeratology contact lens wear[20-24], intracorneal ring segments implantation[25], and radial keratotomy[26].

In keratoconic eyes, epithelial thickness in the

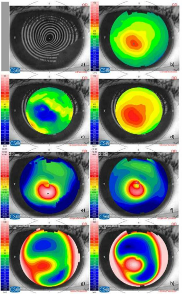

***Figure 7.** Maps of a keratoconic eye. From top left corner: epithelial thickness, stromal thickness, corneal pachymetry, keratoscopy, anterior tangential curvature, posterior tangential curvature, anterior elevation, posterior elevation.*

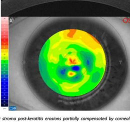

Figure 8. Anterior stroma post-keratitis erosions partially compensated by corneal epithelium increased thickness. Corneal epithelium compensating stromal defects a long time after superficial keratitis did help re-establishing acceptable vision in this case. Recognizing the situation (a) and obtaining a detailed map of its thickness distribution (b), is critical in avoiding unpleasant surprises when planning refractive laser surgery.

region of the cone has been reported to be thinner than that of normal eyes[27-29]. It has also been shown that the epithelial thickness profile across the central 8 mm diameter follows a doughnut pattern characterized by a thinning region over the cone surrounded by an annulus of thickening[8,30].

Before the advent of OCT, several technologies such as confocal microscopy[31] or ultrasound were used to measure epithelial thickness. In some studies, these methods were adopted to measure the average central epithelium thickness. Very-high frequency ultrasound was also used to map the corneal epithelium and stromal thickness over a wide area. However, this technology is not patient-friendly as it requires immersion of the eye in a coupling fluid and thus three-dimensional epithelial mapping still remains unfulfilled in daily routine practice.

Optical coherence tomography is the most recent technology applied to measure the corneal epithelium. It is a non-contact technique, having a high axial resolution that obtains excellent delineation of corneal surfaces and in its Fourier domain version is fast enough to acquire images of a sufficient number of meridians to create a corneal epithelial thickness map[32].

The MS-39 takes advantage of the previous features and offers the user the corneal epithelial and stromal thickness maps in addition to the corneal total thickness map along with the other classical curvature and height maps of the anterior and posterior corneal surfaces. The comprehensive mapping of corneal layers makes the MS-39 a powerful tool to help the clinician in the pre-operative (Figure 8) and post-operative assessment of corneal conditions (Figure 9).

ACKNOWLEDGMENTS

The authors would like to thank David Biggins for the careful review of their manuscript.

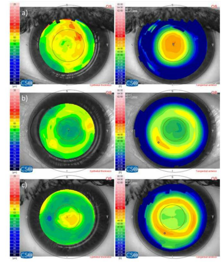

Figure 9. *Epithelial maps and corneal refractive treatments. a) A hyperopic treatment ablates more in the periphery than in the center so that the central stroma becomes a "hill" surrounded by a circular "valley". the epithelium will be thinner over the hill and thicker along the valley. b) In a myopic laser treatment, the central corneal "hill" gets flattened, almost converted into a "valley", in which the epithelium becomes thicker in the center. c) In a myopic orthokeratologic treatment the stroma is not affected, while the rigid gas permeable contact lens modifies transiently the epithelium thickness, making it thicker paracentrally, thereby inducing a central flattening of the anterior corneal curvature.*

REFERENCES

1. *Fercher AF, et al. In-vivo dual-beam optical coherence tomography. In: Europto Biomedical Optics' 93. International Society for Optics and Photonics. 1994.*
2. *Fercher AF, et al. Measurement of intraocular distances by backscattering spectral interferometry. Opt Commun. 1995;117(1):43–8.*
3. *Huang D, et al. Optical coherence tomography. Science. 1991;254(5035):1178–81.*
4. *Swanson EA, et al. In vivo retinal imaging by optical coherence tomography. Opt Lett. 1993;18(21):1864–6.*
5. *Drexler W, et al. Ultrahigh-resolution ophthalmic optical coherence tomography. Nat Med. 2001;7(4):502–7.*
6. *Chinn SR, Swanson EA, Fujimoto JG. Optical coherence tomography using a frequency-tunable optical source. Opt Lett. 1997;22(5):340–2.*
7. *Reinstein DZ, Archer T. Combined Artemis very high-frequency digital ultrasound-assisted transepithelial phototherapeutic keratectomy and wavefront-guided treatment following multiple corneal refractive procedures. J Cataract Refract Surg. 2006; 32:1870–1876.*
8. *Reinstein DZ, Archer TJ, Gobbe M. Corneal epithelial thickness profile in the diagnosis of keratoconus. J Refract Surg. 2009; 25:604–610.*
9. *Reinstein DZ, Silverman RH, Trokel SL, Coleman DJ. Corneal pachymetric topography. Ophthalmology. 1994; 101:432–438.*
10. *Lohmann CP, Patmore A, Reischl U, Marshall J. The importance of the corneal epithelium in excimer-laser photorefractive keratectomy. Ger J Ophthalmol. 1996; 5:368–372.*
11. *Gauthier CA, Holden BA, Epstein D, Tengroth B, Fagerholm P, Hamberg-Nyström H. Role of epithelial hyperplasia in regression following photorefractive keratectomy. Br J Ophthalmol. 1996; 80:545–548.*
12. *Lohmann CP, Güell JL. Regression after LASIK for the treatment of myopia: the role of the corneal epithelium. Semin Ophthalmol. 1998; 13:79–82.*
13. *Reinstein DZ, Silverman RH, Sutton HF, Coleman DJ. Very high-frequency ultrasound corneal analysis identifies anatomic correlates of optical complications of lamellar refractive surgery: anatomic diagnosis in lamellar surgery. Ophthalmology. 1999; 106:474–482.*
14. *Lohmann CP, Reischl U, Marshall J. Regression and epithelial hyperplasia after myopic photorefractive keratectomy in a human cornea. J Cataract Refract Surg. 1999; 25:712–715.*
15. *Spadea L, Fasciani R, Necozione S, Balestrazzi E. Role of the corneal epithelium in refractive changes following laser in situ keratomileusis for high myopia. J Refract Surg. 2000; 16:133–139.*
16. *Erie JC, Patel SV, McLaren JW, Ramirez M, Hodge DO, Maguire LJ, Bourne WM. Effect of myopic laser in situ keratomileusis on epithelial and stromal thickness: a confocal microscopy study. Ophthalmology. 2002; 109:1447–1452.*
17. *Reinstein DZ, Ameline B, Puech M, Montefiore G, Laroche L. VHF digital ultrasound three-dimensional scanning in the diagnosis of myopic regression after corneal refractive surgery. J Refract Surg. 2005; 21:480–484.*
18. *Patel SV, Erie JC, McLaren JW, Bourne WM. Confocal microscopy changes in epithelial and stromal thickness up to 7 years after LASIK and photorefractive keratectomy for myopia. J Refract Surg. 2007; 23:385–392.*
19. *Reinstein DZ, Srivannaboon S, Gobbe M, Archer TJ, Silverman RH, Sutton H, Coleman DJ. Epithelial thickness profile changes induced by myopic LASIK as measured by Artemis very high-frequency digital ultrasound. J Refract Surg. 2009; 25:444–450.*
20. *Reinstein DZ, Gobbe M, Archer TJ, Couch D, Bloom B. Epithelial, stromal and corneal pachymetry changes during orthokeratology. Optom Vis Sci. 2009; 86:E1006–E1014.*
21. *Swarbrick HA, Wong G, O'Leary DJ. Corneal response to orthokeratology. Optom Vis Sci. 1998; 75:791–799.*

22. *Lu F, Simpson T, Sorbara L, Fonn D. Malleability of the ocular surface in response to mechanical stress induced by orthokeratology contact lenses. Cornea. 2008; 27:133–141.*
23. *Sridharan R, Swarbrick H. Corneal response to short-term orthokeratology lens wear. Optom Vis Sci. 2003; 80:200–206.*
24. *Haque S, Fonn D, Simpson T, Jones L. Epithelial thickness changes from the induction of myopia with CRTH RGP contact lenses. Invest Ophthalmol Vis Sci. 2008; 49:3345–3350.*
25. *Reinstein DZ, Srivannaboon S, Holland SP. Epithelial and stromal changes induced by intacs examined by three-dimensional very high-frequency digital ultrasound. J Refract Surg. 2001; 17:310–318.*
26. *Lovisolo, CF.; Mularoni, A.; Calossi, A.; Stewart, CW. Complications of refractive keratotomy. In: Alio, J.; Azar, DT., editors. Management of Complications in Refractive Surgery. Springer-Verlag; Berlin, Germany: 2008. p. 197-224.*
27. *Scroggs MW, Proia AD. Histopathological variation in keratoconus. Cornea. 1992; 11:553–559.*
28. *Haque S, Simpson T, Jones L. Corneal and epithelial thickness in keratoconus: a comparison of ultrasonic pachymetry, Orbscan II, and optical coherence tomography. J Refract Surg. 2006; 22:486–493.*
29. *Aktekin M, Sargon MF, Cakar P, Celik HH, Firat E. Ultrastructure of the cornea epithelium in keratoconus. Okajimas Folia Anat Jpn. 1998; 75:45–53.*
30. *Reinstein DZ, Gobbe M, Archer TJ, Silverman RH, Coleman DJ. Epithelial, stromal, and total corneal thickness in keratoconus: three-dimensional display with Artemis very high-frequency digital ultrasound. J Refract Surg. 2010; 26:259–271.*
31. *Petroll WM, Goldberg D, Lindsey SS, Kelley PS, Cavanagh HD, Bowman RW, Parmar DN, Verity SM, McCulley JP. Confocal assessment of the corneal response to intracorneal lens insertion and laser in situ keratomileusis with flap creation using IntraLase. J Cataract Refract Surg. 2006; 32:1119–1128.*
32. *Li, Yan et al. "Corneal Epithelial Thickness Mapping by Fourier-Domain Optical Coherence Tomography in Normal and Keratoconic Eyes." Ophthalmology 119.12 (2012): 2425–2433. PMC. Web. 17 May 2018.*

CLINICAL CASES

OBSERVATIONS AND ANALYSIS

INDEX

1

CORNEAL INLAYS

MARCO FANTOZZI, M.D. - MASSIMO MAMMONE, M.D.
Ophthalmic Operative Unit "Casa di Cura Barbantini" - Lucca, Italy

To date, there is no optimal solution, nor a gold standard technique, for the correction of presbyopia. Various methods have been proposed over time in order to restore vision at near without affecting distance vision. Among cornea-based methods, PresbyLasik is designed to create multifocal corneas with zones for near, far and intermediate vision using corneal aberration. Laser-assisted monovision provides near vision by partial myopic undercorrection in the non-dominant eye and a complete correction of the visual defect in the dominant eye. Lens-based methods include multifocal IOLs (diffractive, refractive, EDOF) and accommodative IOLs, which modify their dioptric power by contraction of the capsular bag. Finally, intracorneal lenses, commonly known as corneal inlays, are a valid alternative for emmetropic presbyopic patients.

Depending on the design, the operating principle is clearly different:

- Inlays that exploit the pinhole effect to increase depth of focus;
- Inlays that modify the central curvature of the cornea by increasing negative spherical aberration (central hyperprolation of the cornea);
- Lenses with a true refractive effect, adding a positive spherical power (+ 1.25D / + 3.5D).

In all the cases, the implant is always performed only on the non-dominant eye and on emmetropic patients. In this chapter, we will deal with the last type of inlay just described and we will see how OCT can help us achieving a greater understanding of the minor diffractive problems described by patients.

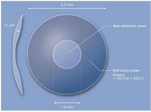

Figure 1. *Presbia corneal inlay.*

The Flexivue corneal lens (Presbia) is a microlens with a diameter of 3.2 mm, made of an inert acrylic material. It has a 1.6 mm central hole that allows intrastromal metabolic exchanges. While the central zone is optically neutral, the refractive peripheral zone provides add powers between +1.25 and +3.5 D (Figure 1). The lens can be implanted into a 250-300 micron corneal pocket created by a femtosecond laser.

As shown by topographic images, no variation of the anterior curvature occurs (keratometry data are unchanged), thanks to the low thickness of the microlens and the small diameter of the corneal tunnel created for implantation (Figure 2).

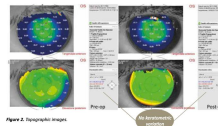

Figure 2. Topographic images.

In Figures 3 and 4 it is possible to clearly highlight the intracorneal lens by scanning AS-OCT.

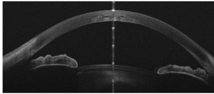

Figure 3. Corneal inlay insertion: post-op image.

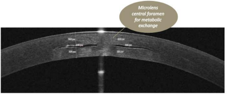

Figure 4. *Corneal inlay insertion: detail.*

The AS-OCT exam highlights how implantation with the iFS femtosecond laser (AMO/Johnson & Johnson) led to a non-homogeneous distension of the lens itself with consequent gull wings-aspect. This anomaly could partly explain the dysphotopsia reported by some patients.
During the applanation phase and consequent "crushing" of the corneal lamellae typical of this technology used, the cornea is stretched and when the applanation is released, the intracorneal pocket develops irregularities.
By using the VisuMax femtosecond laser (ZEISS Meditec AG), which uses a curved applanation cone (therefore more respectful of the true corneal curvature) this gull-wing deformation of the microlens disappears completely, resulting in a regular and homogeneous corneal interface (Figures 5, 6).

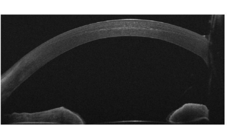

Figure 5. *Post-op check: regular insertion.*

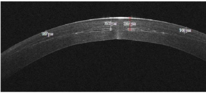

Figure 6. Post-op detail: regular insertion.

The VisuMax laser does not currently have a dedicated software for creating an intracorneal pocket. Therefore we simulated a myopic SMILE (Small Incision Lenticule Extraction) treatment of about 6-7D, which allowed us to use only the back face of the lenticule by ungluing it to the desired depth of about 300 microns, therefore leaving the front face and the typical SMILE cap intact.
In Figure 7 it is possible to highlight, thanks to the high-resolution of the AS-OCT MS-39 of CSO, the geometry of the myopic lenticule cut.

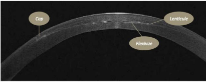

Figure 7. OCT sectional image of a SMILE lenticular cut.

REFERENCES

1. Pallikaris IG, et al. PresbyLASIK approach for the correction of presbyopia. Curr Opin Ophthalmol. 2015;26(4):265272.
2. Labiris G, Toli A, Perente A, Ntonti P, Kozobolis VP. A systematic review of pseudophakic monovision for presbyopia correction. Int J Ophthalmol. 2017 Jun 18;10(6):992-1000.
3. Zare Mehrjerdi MA, Mohebbi M, Zandian M. Review of Static Approaches to Surgical Correction of Presbyopia. J Ophthalmic Vis Res. 2017 Oct-Dec;12(4):413-418. doi: 10.4103/jovr.jovr_162_16. Review.

CASE 1

2

EPITHELIAL INGROWTH AFTER LASER REFRACTIVE SURGERY

MARCO FANTOZZI, M.D. - MASSIMO MAMMONE, M.D.
Ophthalmic Operative Unit "Casa di Cura Barbantini" - Lucca, Italy

Epithelial ingrowth (EI), although rare, is certainly a very bothersome complication of intrastromal laser surgery, both for the surgeon and the patient. It may be secondary to both LASIK and SMILE (Small Incision Lenticule Extraction).

The incidence of visually significant epithelial ingrowth is less than 1% in primary treatments using the microkeratome, but can be around 2% in cases of refractive enhancement (lifting of the preexisting flap).[1-2]

However, the incidence seems to be lower with the creation of the femtosecond laser-assisted flap.[3-4] The ingrowth of epithelial cells in the corneal stromal interface is usually asymptomatic, however it may lead to decreased vision due to induced corneal astigmatism or when the visual axis is involved. In extreme cases, it may result in melting of the overlying flap.

Treatment is generally necessary in case of decreased vision or threat of flap melting.

Probst and Machat[5] have tried to classify epithelial ingrowth as follows:

Grade 1: thin ingrowth, 1-2 cells thick, limited to within 2 mm of flap edge, transparent, difficult to detect, well-delineated white line along advancing edge, no associated flap changes, non-progressive. (No treatment required)

Grade 2: thicker ingrowth, discrete cells evident within the nest, at least 2 mm from flap edge, individual cells translucent, easily seen on slit lamp, no demarcation line along the nest, corneal flap edge rolled or grey, no flap edge melting or erosion, usually progressive. (Requires non-urgent treatment within 2-3 weeks)

Grade 3: pronounced ingrowth, several cells thick, greater than 2 mm from flap edge, ingrowth areas appear opaque, obvious on slit lamp, white geographic areas of necrotic epithelial cells without a demarcation line, corneal flap margins rolled with thickened white-greyish appearance. Progression results in large areas of flap melting from collagenase release from necrotic epithelium. Confluent haze develops peripheral to the flap edge while the flap pulls away, leaving exposed stromal bed in contact with surface epithelium. (Urgent treatment required with close follow-up due to frequent recurrences).

Elective treatment, when required, consists in relifting the flap and scraping the epithelial cell plaque both from the stromal bed and from the flap interface, with final application of a therapeutic contact lens.

In case of recurrence, useful treatment options might be diluted ethyl alcohol, mitomycin or phototherapeutic keratectomy (PTK), taking into account that complications may occur.

Although easy to diagnose with simple observation at the slit lamp, the picture of epithelial ingrowth may be confused with a simpler and self-resolving picture of localized "rearrangement" of the corneal epithelium (focal epithelial hyperplasia, basal membrane dystrophy), as it can be observed in the following images.

For differential diagnosis, it is useful to perform a scan using AC-OCT which will be able to highlight the exact location of the anomaly.

In case of true EI, the hyperdense area will be present under the LASIK flap or the SMILE cap, while in the case of pseudo-EI, the hyperdense area will be located above the Bowman's membrane.

Pseudo epithelial ingrowth requires no treatment, as it resolves spontaneously. An accurate differential diagnosis is therefore mandatory.

Case A

Patient after SMILE for the correction of myopia and astigmatism was visited 7-10 days after the procedure due to complaints of visual discomfort. Slit lamp examination showed a clinical picture similar to that of classic EI (Figure 1).

Because the lesion laid over the center of the pupil, therapy consisted in re-lifting the flap and removing the epithelial plaque. More thorough examination by AS-OCT showed that the hyperdense area was not beneath the SMILE cap but above Bowman's membrane (pseudo-epithelial ingrowth) (Figure 2).

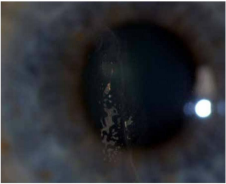

Figure 1. *Pseudo-epithelial ingrowth: slit lamp image.*

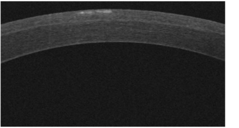

Figure 2. *Pseudo-epithelial ingrowth: OCT sectional image.*

In Figure 3, complete spontaneous resolution at the second month of follow-up can be seen. It can also be observed how the typical SMILE cap-line is already more tenuous and less centralized in the second month of follow-up.

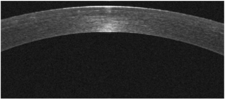

Figure 3. *Second moth follow-up after SMILE.*

CASE 2

Case B
Patient after hyperopic LASIK complained of continuous ocular discomfort and foreign body sensation. In Figure 4 a true case of EI (very similar to the scenario in Figure 1) can be observed.

Figure 4. *Post lasik epithelial ingrowth: slit lamp view.*

Although the epithelial ingrowth did not create problems of irregular astigmatism due to being very peripheral and out of the visual axis, it was necessary to proceed with re-lifting the flap and scraping the epithelial plaque in order to avoid possible corneal melting (Figure 5).

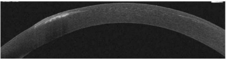

Figure 5. *Irregular course of the flap due to underlying epithelial ingrowth.*

AS-OCT shows epithelial ingrowth underneath the LASIK flap, causing an irregularity in its course and a thinning of the overlying epithelium.
In conclusion, it is mandatory to detect the exact location of suspect epithelial ingrowth by examining corneal OCT. Though rare and infrequent, anomalies that simulate a picture of EI (pseudo Epithelial Ingrowth) may lead to misdiagnosis.
While true cases of Epithelial Ingrowth can benefit from surgical treatment, pseudo epithelial ingrowth requires no intervention and spontaneously resolves over time.

REFERENCES

1. *Wang MY, Maloney RK. Epithelial ingrowth after laser in situ keratomileusis. Am J Ophthalmol. 2000 Jun; 129(6): 746-51.*
2. *Asano-Kato N, Toda I, Hori-Komai Y, et al. Epithelial ingrowth after laser in situ keratomileusis: clinical features and possible mechanisms. Am J Ophthalmol. 2002 Dec; 134(6): 801-7.*
3. *Kamburoglu G, Ertan A. Epithelial ingrowth after femtosecond laser-assisted in situ keratomileusis. Cornea. 2008 Dec; 27(10): 1122-5.*
4. *Letko E, Price MO, Price FW Jr. Influence of original flap creation method on incidence of epithelial ingrowth after LASIK retreatment. J Refract Surg. 2009 Nov; 25(11): 1039-41. doi: 10.3928/1081597X-20090617-13. Epub 2009 Nov 13.*
5. *Machat JJ, Slate S, Probst SE. The Art of LASIK, 2nd ed. Thorofare, NJ SLACK; 1999. 427-33.*
6. *Haw WW, Manche EE. Treatment of progressive or recurrent epithelial ingrowth with ethanol following laser in situ keratomileusis. J Refract Surg. 2001 Jan-Feb; 17(1): 63-8.*

3

ICL INTRAOPERATIVE INVERSION

ANDREA BEDEI, M.D.
Studi Oculistici - Lucca, Italy

The Visian implantable collamer lens (ICL, STAAR Surgicasl Co. Switzerland) is a foldable posterior chamber phakic intraocular lens. It represents an excellent option for vision correction in patients who are not ideal candidates for laser vision correction. The ICL is a rectangular micro-thin lens made of collamer, a biocompatible material. This lens is foldable and can be injected through an incision of 3.2 mm. Once delivered into the anterior chamber the four footplates of the lens are placed under the iris into the sulcus. A possible surgical complication could be an inverted insertion of the ICL (Upside-down). This accidental intraoperative inversion can cause an incorrect and incomplete correction of the visual defect, as well as dispersion of pigment from the posterior face of the iris by direct contact. While this condition may be difficult to recognize by slit lamp observation, it may be easier to see it through OCT imaging of the anterior segment (Figure 1). In the OCT image, we can observe an inversion of the concavity of the lens (Figure 2) that causes an anterior displacement and a deflection of the iris at the point where the ICL touches its posterior face (Figure 1).

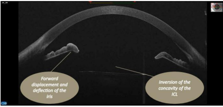

Figure 1. *Incorrect position of the ICL.*

Figure 2. Zoom of the portion of the image containing the ICL.

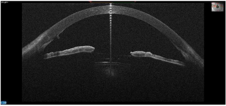

Figure 3. Correct position of the ICL.

TAKE HOME MESSAGE

The high resolution scans provided by MS-39 enable easy recognition of the correct positioning of an ICL.

REFERENCES

1. *Kumar DA, Agarwal A, Prakash G, Sivanganam S, Jacob S, Agarwal A. Viscocannula-assisted reinversion of implantable collamer lens: comparison of postoperative outcomes with the fellow eyes. Am J Ophthalmol. 2012 Jan;153(1):62-7*

4

SALZMANN'S NODULAR DEGENERATION

ANDREA BEDEI, M.D.
Studi Oculistici - Lucca, Italy

Salzmann's nodular degeneration is a slowly progressive condition in which gray-white to bluish elevated nodules measuring 1-3 mm are seen anterior to the Bowman's layer of the cornea, usually bilaterally and located near the limbus or in the mid-peripheral cornea (Figure 1). These nodules consist of a hypercellular area of extracellular matrix seen between a thinned overlying corneal epithelium and a fragmented or absent Bowman's layer (Figure 2), in addition to disorganized subepithelial collagen fibrils. Both the cause and the pathogenetic mechanism are mysterious, so much so that many believe it is not a single entity.
Seventy-two to 88% of cases occur in females. Many eyes with this degeneration are asymptomatic. Usually there are no disturbances up until the advanced stages of the disease, when recurrent corneal erosions can occur with consequent ocular inflammation, photophobia, blepharospasm, lachrymation and decreased visual acuity. Spontaneous resolution has not been reported to date. Treatment can be medical or surgical depending on the clinical picture. Medical management may include ocular lubrication, steroid eye drops, warm compresses and proper eyelid hygiene. Steroid use must be strictly controlled. Surgical management is taken into consideration when there is a serious ocular discomfort or a reduced visual acuity due to irregular astigmatism. Superficial keratectomy, sometimes associated with PTK, is effective in 90% of cases. In 10-15% of eyes recurrences may occur after several years.

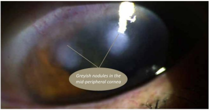

***Figure 1.** Salzmann's nodular degeneration: slit lamp view.*

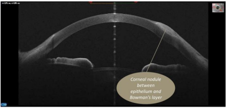

Figure 2. *The 16 mm section image shows the exact location of the corneal nodules.*

TAKE HOME MESSAGE

The high resolution scans provided by MS-39 allow detection of the exact location of the nodules, found between a thin corneal epithelium and Bowman's membrane.

REFERENCES

1. *Roszkowska AM, Aragona P, Spinella R, Pisani A, Puzzolo D, Micali A. Morphologic and Confocal Investigation on Salzmann Nodular Degeneration of the Cornea. 2011; 52(8): 5910-5919.*
2. *Hamada S, Darrad K, McDonnell P. Salzmann's Nodular Corneal Degeneration: Clinical Findings, Risk Factors, Prognosis and the Role of Previous Contact Lens Wear. Contact lens and Anterior Eye. 2011 Aug; 34(4): 173-8.*
3. *Eberwein P, Hiss S, Auw-Haedrich C, Sundmacher R, Hauer K, Boehringer D, Meier P, Reinhard T. Epithelial Marker Expression in Salzmann Nodular Degeneration Shows Characteristics of LimbalTransient Amplifying Cells and Alludes to an Involvement of the Epithelium in its Pathogenesis. ActaOphthalmologica. 2010 88: e184–e189.*
4. *Graue-Hernández EO, Mannis MJ, Eliasieh K, Greasby TA, Beckett LA, Bradley JC, Schwab IR. Salzmann Nodular Degeneration. Cornea. 2010; 29(3): 283-9.*
5. *Stone D, Astley R, Shaver R, Chodosh J. Histopathology of Salzmann Nodular Corneal Degeneration. Cornea. 2008; 27(2): 148-51.*
6. *Farjo AA, Halperin GI, Syed N, Sutphin JE, Wagoner MD. Salzmann's Nodular Corneal Degeneration Clinical Characteristics and Surgical Outcomes. Cornea. 2006; 25(1): 11-5.*

5

DESCEMET MEMBRANE ENDOTHELIAL KERATOPLASTY (DMEK)

STANDARD CASE AND SPECIAL SITUATIONS

JORGE L. ALIÓ DEL BARRIO, M.D., PhD
Vissum Corporación & Universidad Miguel Hernández - Alicante, Spain

Descemet Membrane Endothelial Keratoplasty (DMEK) has become the gold standard surgical treatment for corneal endothelial diseases in order to restore corneal transparency and so the visual function. A DMEK graft is composed of only two layers (Descemet membrane and endothelium), so the donor tissue is less than 20 micron thick. This extremely low thickness makes the graft hardly visible from the slit lamp during the postoperative period. A high resolution anterior segment AS-OCT is essential in order to monitor the proper adherence, orientation and health of the implanted donor tissue.

MS-39 presents the highest image resolution among all commercially available AS-OCT, being this point critical for any corneal surgeon.

1. STANDARD DMEK

After a successful DMEK, the graft can hardly be identified, although during the first few postoperative days, there are usually limited detachments in the extreme periphery of the graft, where the DMEK can still be seen (Figure 1).

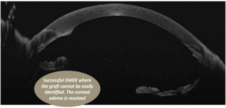

Figure 1. *Successful DMEK.*

2. MINOR GRAFT DETACHMENTS

During the early postoperative period after DMEK, limited peripheral detachments are common, and do not require any intervention since they usually resolve spontaneously (Figure 2).

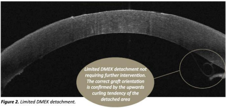

Figure 2. Limited DMEK detachment.

3. LARGE GRAFT DETACHMENTS

Large detachments involving more than 1/3 of the extension of the DMEK graft require a new injection of air or gas into the anterior chamber in order to enhance the adherence of the graft (Figure 3).

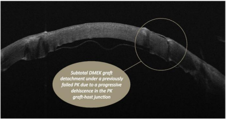

Figure 3. Subtotal DMEK graft detachment under previously failed PK.

An inadequate host descemetorrhexis before graft implantation will leave host DM remnants that will interfere with the adherence of the donor tissue, inducing detachments that will hardly respond to new anterior chamber air injections. These host DM remnants can only be identified with the highest AS-OCT image resolution (Figure 4).

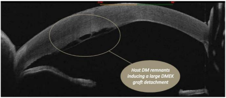

Figure 4. *Host DM remnants.*

4. UPSIDE DOWN GRAFT

If the donor DMEK tissue is implanted upside down (endothelial side upwards), the recipient corneal stroma clearance will not improve and large graft detachments will commonly be identified, where the detached tissue will abnormally curl downwards (while a detachment in a correctly positioned DMEK graft will curl upwards) (Figure 5).

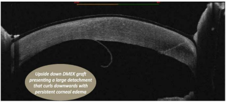

Figure 5. *Upside down DMEK graft.*

5. DMEK UNDER DMEK

DMEK can be used as well to restore the corneal transparency of previous DMEK secondary failures without the need of removing the first DMEK graft (in the case that it was previously anatomically and functionally normal). Thanks to the high resolution of the MS-39, both old and new DMEK grafts can be differentiated (Figures 6, 7, 8).

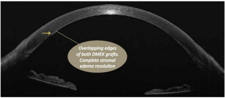

Figure 6. *DMEK under DMEK.*

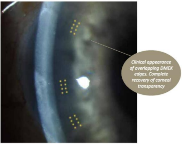

Figure 7. *DMEK under DMEK: clinical appearance of overlapping DMEK edges.*

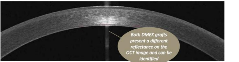

Figure 8. *DMEK under DMEK.*

6. DMEK UNDER PK

Currently, transparency from failed penetrating keratoplasties can be restored with DMEK, allowing a faster visual recovery and restoration of pre-failure visual function, thus avoiding all potential drawbacks of a new penetrating graft (rejection, slow visual recovery, refractive change, glaucoma, etc) (Figures 9, 10, 11).

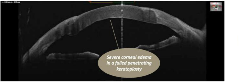

Figure 9. *Severe corneal edema due to a failed PK.*

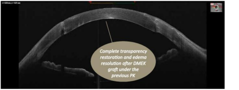

Figure 10. *Complete transparency restoration and edema resolution after DMEK.*

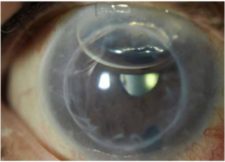

Figure 11. Slit lamp picture one week after DMEK under PK graft. Transparency is fully recovered.

7. DMEK UNDER DLEK

For those patients presenting endothelial dysfunction together with posterior stromal scars with a healthy anterior stroma, femtosecond laser assisted DLEK (deep lamellar endothelial keratoplasty) and DMEK graft techniques can be combined in order to restore corneal transparency and vision, while avoiding penetrating keratoplasty (Figures 12, 13).

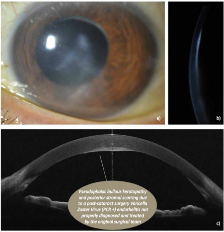

Figure 12. *Slit lamp and OCT images show a bullous keratopathy*

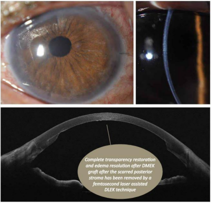

***Figure 13.** Slit lamp and OCT images show a complete transparency restoration and edema resolution.*

TAKE HOME MESSAGE

A high resolution AS-OCT such as the MS-39 is an essential tool for any corneal surgeon. Its high definition allows accurate diagnosis, surgical planning and postoperative follow-up of all corneal disorders.

The extreme low thickness of DMEK grafts makes them almost clinically invisible for the surgeon, giving AS-OCT a critical role in the postoperative management of such patients.

REFERENCES

1. *Melles GR, Ong TS, Ververs B, et al. Descemet membrane endotelial keratoplasty (DMEK). Cornea 2006; 25:987–990.*
2. *Alió del Barrio JL, Vega-Estrada A, Alió JL. Descemet Membrane Endothelial Keratoplasty (DMEK) Under Previous DMEK for Secondary Endothelial Graft Failure. Cornea 2018; 37(6): 793-795.*
3. *Alió del Barrio JL, Ziaei M, Bhogal M, Allan BD. Femtosecond Laser-Assisted Deep Lamellar Endothelial Keratoplasty: a new approach to a forgotten technique. Cornea 2015; 34:1369-74.*

6

FUCHS' DYSTROPHY

FROM FIRST CHANGES TO BULLOUS KERATOPATHY

CLAUDIO MACALUSO, M.D.
University of Parma and National Research Council- Parma, Italy

Fuchs' dystrophy is a usually bilateral, slowly progressing form of corneal dystrophy. It affects the corneal endothelium with accumulation of focal drop-like thickenings of the Descemet membrane called guttae (gutta = drop). These anomalies cause a progressive endothelial cell functionality loss, leading to corneal edema and loss of vision.
In all the stages of the disease, MS-39 allows detection of subtle corneal modifications, from endothelium to epithelium.

1. TRACES: CORNEA GUTTATA

In mild cases of Fuchs' dystrophy both the corneal epithelium and stroma are normal, while the endothelial layer is abnormally thickened, hyper-reflective, with minor profile irregularities due to the development of guttae. At this initial stage of the disease, endothelial guttae only induce minor visual changes due to light scattering, and the endothelial pump is not significantly affected (Figure 1, 2).

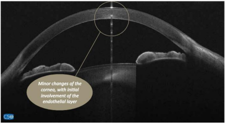

***Figure 1.** Fuchs' dystrophy: early stage 16 mm image.*

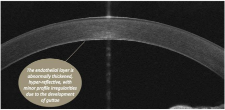

Figure 2. *8 mm section image of an initial stage of Fuchs' corneal dystrophy (cornea guttata).*

2. MILD: INITIAL STROMAL CHANGES

As the endothelial pump starts to become compromised, the stroma becomes thicker and less transparent, affecting vision in a more significant way. When this condition lasts for a sufficient period of time, the subepithelial stroma loses its transparency, showing a haze-like appearance on slit lamp examination (Figures 3, 4, 5, 6).

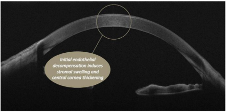

Figure 3. *16 mm section image of a mild stage of Fuchs' corneal dystrophy: evident stromal thickening.*

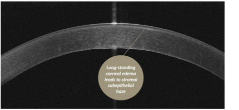

Figure 4. *8 mm section image of a mild stage of Fuchs' corneal dystrophy with first stromal changes.*

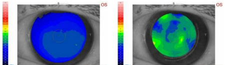

Figures 5-6. *Maps showing the increased thickness of the whole corneal structure and the irregular thickness of the epithelial layer.*

3. MODERATE: SIGNIFICANT STROMAL CHANGES + EARLY BULLOUS KERATOPATHY

As the disease progresses, stromal swelling increases further. The transparency of both stroma and epithelium is compromised, endothelial folds and epithelial thickening with bullae appear (Figures 7, 8).

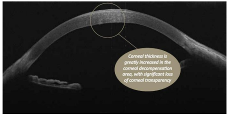

Figure 7. *16 mm section image in a moderate stage of Fuchs' corneal dystrophy significantly affecting all corneal layers.*

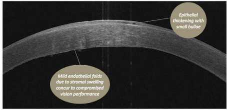

Figure 8. *8 mm section image in a moderate stage of Fuchs' corneal dystrophy significantly affecting all corneal layers.*

4. SEVERE: BULLOUS KERATOPATHY

Further failure of the endothelial pump leads to major transparency loss, larger endothelial folds and bullous epithelial modifications (Figures 9, 10, 11).

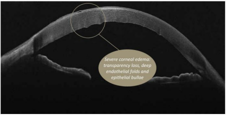

Figure 9. *16 mm section images of a severe bullous keratopathy case.*

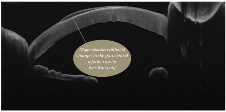

Figure 10. *16 mm section images of a severe bullous keratopathy case.*

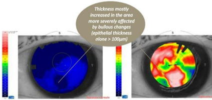

Figure 11. Maps showing the highly increased thickness of the whole corneal structure and the irregular thickness of the epithelial layer.

TAKE HOME MESSAGE

Through all the stages of corneal decompensation, the high resolution scans provided by MS-39 allow detection of subtle corneal modifications, endothelium to epithelium.
The subepithelial, haze-like, stromal opacities often do not completely reverse after endothelial transplantation, thus reducing the recovery of visual function. Early detection and monitoring of these modifications are mandatory in order to allow for timely surgical intervention.

7

CORNEAL MACULAR DYSTROPHY

RITA MENCUCCI, M.D. - MICHELA CENNAMO, M.D. - ELEONORA FAVUZZA, M.D.
Eye Clinic, Department of Surgery and Translational Sciences, University of Florence
Florence, Italy

Macular corneal stromal dystrophy is a bilateral hereditary autosomal recessive dystrophy, characterized by mucopolysaccarides deposition in the corneal stroma. Generally, it develops during the teenage years, evolving to vision loss by the third decade of life. In its later stages, it may involve almost all of the corneal layers, including Descemet membrane and endothelium. The affected corneas are usually thinner than normal.

Figure 1 shows a cornea of a 45 year-old affected patient (right eye, BCVA 0.2) with irregular, not well-demarcated opacities without vascularization, that are distributed from limbus to limbus. Unlike granular corneal dystrophies, no clear corneal areas can be evidenced between the opacities.

Figure 1. *Corneal macular dystrophy: frontal slit lamp image.*

In these types of irregular corneas, the MS-39 was able to provide a wide range of information: corneal topography maps (Figure 2) show a central corneal thickness of 437 microns, irregular anterior and posterior corneal surfaces, and a notable inhomogeneous epithelial thickness.

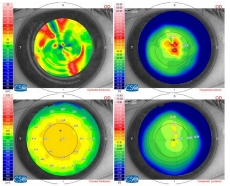

Figure 2. Corneal topographic maps.

Figure 3 represents the corneal AS-OCT section (MS-39): hyperreflective stromal deposits are detectable in the subepithelial area, mainly found in the anterior stroma, and only partially noted in the posterior stroma. The whole stroma is diffusely hyperreflective.

CASE 7

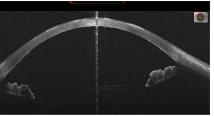

Figure 3. Corneal macular dystrophy 16 mm image.

The deposits distribution pattern within the corneal stroma can be a guide for surgical options. In these cases, a penetrating keratoplasty (PK) is generally indicated. However, if the deposits are mainly located in the anterior corneal stroma and confocal microscopy shows a normal endothelium, a deep anterior lamellar keratoplasty (DALK) can be planned, characterized by a lower risk of immune rejection and by the possibility to retain the healthy endothelium of the young patient.

TAKE HOME MESSAGE

The MS-39 can guide our surgical approach by providing us with important information beyond the clinical appearance at the slit lamp examination: the epithelial and subepithelial irregularities, corneal pachymetry (not easy to obtain by Scheimpflug camera in these cases) and the depth of the stromal opacities.

REFERENCES

1. *Aggarwal S, Peck T, Golen J, Karcioglu ZA. Macular Corneal Dystrophy: A Review. Surv Ophthalmol. 2018 Mar 28. pii: S0039-6257(17)30101-7. doi: 10.1016/j.survoph, dithal.2018.03.004. [Epub ahead of print]*

8

BAND KERATOPATHY

RITA MENCUCCI, M.D. - MICHELA CENNAMO, M.D. - ELEONORA FAVUZZA, M.D.
Eye Clinic, Department of Surgery and Translational Sciences, University of Florence
Florence, Italy

Band keratopathy is a calcific degeneration of the superficial cornea. It can be either idiopathic or caused by chronic ocular inflammations (e.g. uveitis or keratitis), hypercalcemia, hyperphosphoremia, corneal exposure to silicon oil (e.g. aphakic eye), or by chronic exposure to mercurial preservatives.
Before its surgical removal, an AS-OCT scan can be useful to evaluate the residual corneal thickness underneath the calcific deposition, even though the presence of calcium may cause a shadowing effect.
In the following case (male patient with chronic exposure to glaucoma medications), the band keratopathy (calcium + epithelial hyperplasia) appears to include the whole epithelium, Bowman's layer and the very anterior part of the stroma. A thin empty space between the banded lesion and the remaining stroma (440 µm) is detectable (Figure 1).
This empty space can act as a surgical cleavage plane during band keratopathy removal (Figure 2).

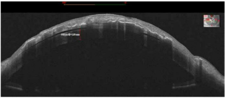

Figure 1. *Band keratopathy: a thin empty space between the banded lesion and the remaining stroma (440 µm) is detectable.*

Figure 2. The empty space can act as a surgical cleavage plane during band keratopathy removal.

CASE 8

TAKE HOME MESSAGE

The MS-39 can provide useful information concerning the corneal tissue below an opacity: the thickness of residual tissue and the presence of a surgical cleavage plane.

REFERENCES

1. *Jhanji V, Rapuano CJ, Vajpayee RB. Corneal calcific band keratopathy. Curr Opin Ophthalmol. 2011 Jul; 22(4): 283-9*

9

EPITHELIAL BASEMENT MEMBRANE DYSTROPHY

EPITHELIAL THICKNESS FOLLOW-UP

GIACOMO SAVINI, M.D.
IRCCS Fondazione G.B. Bietti - Rome, Italy

Epithelial basement membrane (map-dot-fingerprint) dystrophy is a bilateral anterior corneal dystrophy characterized by grayish epithelial fingerprint lines, geographic map-like lines, and dots noted on slit lamp examination. It often leads to recurrent epithelial erosions (Figure 1).

Figure 1. *Slit lamp appearance of an epithelial basement membrane dystrophy case*

Epithelial healing can be followed using anterior segment OCT. In this patient, the epithelial map at presentation showed a marked thickening, which disappeared after 3 months of soft contact lens use. Best corrected visual acuity increased from 20/40 to 20/20 (Figure 2).

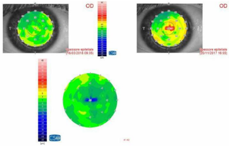

Figure 2. Differential map of epithelial thickness. Top left: the epithelial thickness is within normal limits after 3 months of soft contact lens use. Top right: early appearance of the central epithelial thickening due to recurrent erosions and subsequent healing. Bottom: differential map showing the reduction of central epithelial thickness.

TAKE HOME MESSAGE

Epithelial thickness mapping is a unique technique to confirm the diagnosis of map-dot-fingerprint dystrophy and can be used to follow the course of the disease and the effectiveness of treatments.

10

ICL VAULTING

POSTOPERATIVE EVALUATION OF THE ICL POSITION

GIACOMO SAVINI, M.D.
IRCCS Fondazione G.B. Bietti - Rome, Italy

Implantation of phakic intraocular lenses (IOLs), such as the Implantable Collamer Lens (ICL, Staar), is a commonly used surgical technique to correct refractive errors. Complications are rare and in most cases related to an excessive or insufficient distance between the IOL and the anterior surface of crystalline lens, referred to as vaulting. Excessive vaulting is caused by an oversized ICL and can lead to glaucoma, whereas insufficient vaulting is caused by an undersized ICL and can induce a cataract. Appropriate vaulting values range between 200 and 1000 microns.
Accurate vaulting quantification is difficult with traditional techniques such as Scheimpflug imaging, due to the transparency of the ICL. Anterior segment OCT enables a clear identification of the ICL and measurement of vaulting.

1. NORMAL VAULTING

In this patient the anterior and posterior edges of the ICL are evident on postoperative day 1 in the pupillary area. Central vaulting is 255 microns according to the manual caliper (Figure 1a).

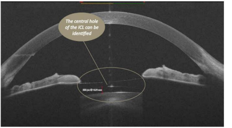

Figure 1a. *Correctly positioned ICL.*

In the same eye on the same day, it is not possible to visualize the edges of the lens with two different Scheimpflug cameras. As a consequence, it is quite difficult to understand if vaulting is appropriate and over- or undersizing of the ICL has been avoided (Figure 1 b-c).

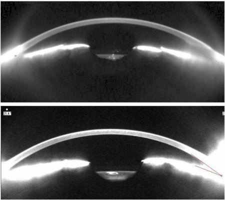

Figure 1 b-c. Images of two different Scheimpflug devices: ICL edges are not visible at all.

2. EXCESSIVE VAULTING

In this patient, who underwent hyperopic ICL implantation, the distance between the ICL and the crystalline lens is borderline, i.e. 1013 microns. As a consequence, the irido-corneal angle may become narrow and intraocular pressure may increase (Figure 2).

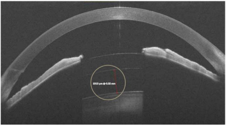

Figure 2. *ICL in hyperopic eye: excessive vaulting.*

TAKE HOME MESSAGE

Since appropriate ICL vaulting is a key factor for the success of this surgical technique, anterior segment OCT is the only method to accurately measure this parameter and to ensure an uncomplicated postoperative follow-up.

11

DYNAMIC GONIOSCOPY

ANGLE CLOSURE IN SCOTOPIC CONDITIONS

ANTONIO MORENO, M.D.
Clínica Oftalmológica Antonio Moreno - Malaga, Spain

This is the case of a 57 year-old male with hyperopia of +2.75 D who presented to our clinic complaining of recurrent frontal and periorbital headaches, without apparent etiology in the screening visit.
Slit lamp examination showed a shallow anterior chamber, but when performing an MS-39 section with dynamic motion capture, angle closure was observed in scotopic conditions. The patient underwent iridotomy in both eyes, with immediate cessation of the migraine symptoms.

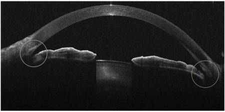

Figure 1. *Section image in photopic light conditions: a narrow but not closed angle is appreciated.*

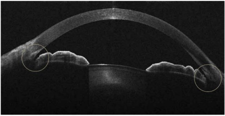

Figure 2. Section image in mesopic light conditions, in which the gradual closing of the angle is observed.

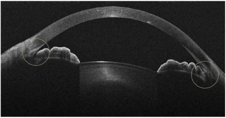

Figure 3. Tomographic section in which angle closure occurring in scotopic conditions is appreciated.

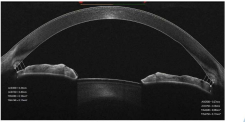

Figure 4. Angle measurements under photopic light conditions.

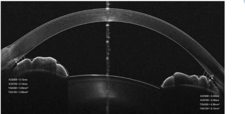

Figure 5. Angle measurements under scotopic light conditions. When the pupil enlarges, angle closure can be observed.

12

PELLUCID MARGINAL DEGENERATION (PMD)

ANTONIO MORENO, M.D.
Clinica Oftalmològica Antonio Moreno - Malaga, Spain

Pellucid marginal degeneration is a rare corneal ectasia characterized by peripheral and progressive corneal thinning. Usually it affects the inferior portion of the cornea, although in rare case it may also affect the superior portion. Pellucid marginal degeneration usually occurs during the third and the fourth decade of life. It is in most cases bilateral and asymmetric, with an increase of against-the-rule astigmatism.

From the topographical point of view, it usually appears as a band of bilateral semilunar increased curvature associated with local thinning, usually from 210° to 330° and 1 mm from the limbus. It differs from keratoconus for both the location and the absence of Fleischer rings and Vogt's striae (Figure 1).

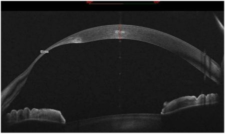

***Figure 1.** Corneal section at 122°, showing the significant thinning at the inferior level (61 µm, vs. 571 µm for the central cornea). The limbal zone is preserved. The epithelium does not seem to be affected in the ectatic zone.*

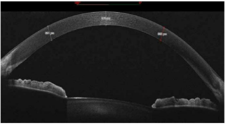

Figure 2. Corneal section at 180° appears as normal in both shape and thickness.

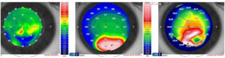

Figure 3. Epithelial thickness, corneal pachymetry and tangential anterior curvature. Epithelial thickness is within normal limits in the ectatic area despite the significant decrease in pachymetry and the notable steepening. The tangential map shows the typical "croissant" or "crab clamp" pattern.

13

LASIK FLAP DISPLACEMENT OCCURRING IN THE EARLY POSTOPERATIVE PERIOD

ANTONIO MORENO, M.D.
Clinica Oftalmològica Antonio Moreno - Malaga, Spain

This is the case of a 34 year-old male with myopia of -4D who underwent LASIK surgery (Figures 1, 2). Twenty-four hours post surgery, the patient showed up with flap displacement in the right eye. After immediate repositioning, an optimal result was achieved both visually and anatomically (Figures 3, 4, 5).

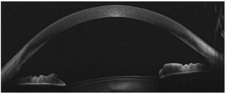

Figure 1. *Pre-operative tomographic section performed at 45°.*

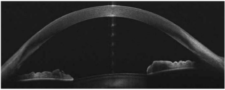

Figure 2. *Tomographic section performed at 45°, 35 minutes after surgery. The regularly shaped flap is shown.*

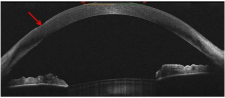

Figure 3. Tomographic section performed at 45°, 24 hours after surgery. The red arrow points at the area of the stroma exposed by the displacement of the flap.

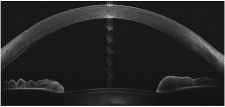

Figura 4. Tomographic section captured after the repositioning of the displaced flap.

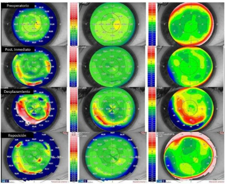

Figure 5. Comparative images of the previous tangential, anterior sagittal and anterior elevation maps acquired with the MS-39 tomographer in the pre-operative and immediate post-operative period, with the flap displaced and after its repositioning.

14

PENETRATING KERATOPLASTY IN PELLUCID MARGINAL DEGENERATION

ANTONIO MORENO, M.D.
Clínica Oftalmològica Antonio Moreno - Malaga, Spain

We present the case of a patient with pellucid marginal degeneration who underwent penetrating keratoplasty due to significant loss of visual acuity.

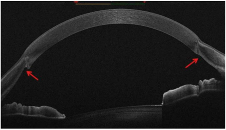

***Figure 1.** Tomographic section performed at 180°, where the transplanted button is noted in great detail, as well as the boundary between it and the recipient peripheral cornea (red arrows).*

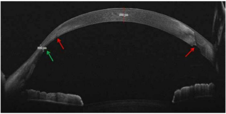

Figure 2. Section performed at 90°. The transition between donor and recipient cornea (red arrows) is clearly visible, as well as the inferior corneal thinning, characteristic of pellucid marginal degeneration (green arrow).

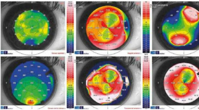

Figure 3. Corneal topographic images mapping epithelial thickness. Anterior sagittal, anterior elevation, pachymetry, anterior tangential and equivalent refractive maps are included.

15

BLEB ANALYSIS IN GLAUCOMA SURGERY

GIAN LUCA LAFFI, M.D., Glaucoma Consultant,
Sant'Orsola-Malpighi Hospital - Bologna, Italy
San Marino Hospital - San Marino, Italy
Studio Oculistico d'Azeglio - Bologna, Italy

1. BLEB AFTER ONE MONTH POST-TRABECULECTOMY

A 67 year-old man with -5D of myopia underwent trabeculectomy with mitomycin C (MMC) and two releasable sutures for a primary open angle glaucoma (POAG) in his right eye. The photo, taken at 1 month post-op with the CSO OCT imaging 1 month postop (Figure 1) shows a well developed bleb with a wide cavity (yellow arrow), a well identifiable Tenon area (red arrow) surrounding the cavity and conjunctiva with small cysts on the anterior and posterior parts of the bleb (blue arrows). It is interesting to observe the aqueous pathway (in black) flowing from the anterior chamber, through the foramen created by a punch and under the flap lifted up close to the Tenon area.

The intraocular pressure (IOP) was 6 mmHg at 1 month after the removal of the flap sutures and 8mmHg after 1 year without glaucoma medication. In this case the CSO AS-OCT highlights the pathophysiology of the bleb and reassures the surgeon about the functioning of the filtration bleb (Figure 1).

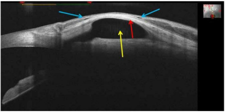

Figure 1. *Bleb after one month post-trabeculectomy with MMC.*

2. TUBE AFTER 3 YEARS: INTRALUMINAL SUTURE THREAD INSITE

A 70-year-old man received three years ago a Molteno3 drainage implant for primary open angle glaucoma (POAG) in his right eye. It is interesting to note the 3-0 nylon suture (yellow arrow) inside the silicon tube of the drainage implant (green brackets). The silicone tube (green brackets) of the drainage implant (white arrow). The silicone tube has an internal lumen of 0.34 mm (blue brackets) and the 3-0 suture (yellow arrow) has a diameter of 0.3 mm. This allows space for drainage also with an inside suture. The CSO OCT effectively shows the aqueous inside the tube (black color – red arrow) inside the tube over the nylon suture (yellow arrow). After 3 years, the IOP is 14 mmHg with a combination of timolol and brinzolamide twice a day (Figure 2).

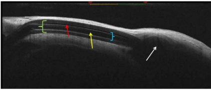

Figure 2. *Molteno drainage.*

3. BLEB 14 DAYS AFTER XEN45 PROCEDURE: CSO OCT MS39 INDICATES A BAD PROGNOSIS

A 55 year-old man underwent a combo phaco-XEN45 implant for primary open angle glaucoma (POAG) in his left eye. After two weeks the IOP was 16mmHg, with a well formed

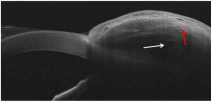

Figure 3. *XEN45: bleb 2 weeks after implant.*

hyperemic bleb. CSO OCT clearly shows the failure of this bleb (Figure 3), as it highlights a very thick and compact Tenon area (red arrow) and a very deep XEN45 implant (white arrow). During the follow-up, the reduction of conjunctival cysts and bleb volume was detected and associated with an IOP increase. Two months after the XEN45 implant, the patient underwent bleb revision due to reduced drainage from fibrosis.

4. BLEB 3 MONTHS AFTER XEN45 MS-39 PROCEDURE: CSO OCT MS39 INDICATES A GOOD PROGNOSIS

A 79 year-old man received a XEN45 implant for primary open angle glaucoma (POAG) in his left eye. Three years prior to the surgery he underwent a phacoemulsification with IOL implantation. This 3 months post-op scan (Figure 4), shows a good volume with a hyporeflective cavity with trabeculae (yellow arrow) and normal thick Tenon area (red arrow) and conjunctival cysts (blue arrow). The IOP was 9 mmHg and remained stable after six months. The CSO OCT shows a well-functioning bleb with only slight fibrosis. OCT is able to identify the correct positioning of the XEN45 under the conjunctiva. It is also able to show the internal (45 micron) (white arrow) and the external (150 micron) XEN45 lumen (blue brackets).

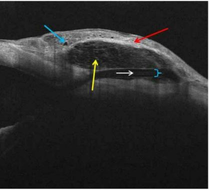

***Figure 4.** Phaco, IOL in PC, XEN45 inplant: 3 months follow-up.*

16

CORNEAL EPITHELIAL THICKNESS CHANGES AFTER LASER REFRACTIVE SURGERY

NORMAL AND DIFFICULT CASES

FRANCESCO CARONES, M.D.
Carones Vision- Milan, Italy

The reshaping of the anterior corneal curvature with lasers allows for the correction of refractive errors in a very predictable way. Procedures like laser in situ keratomileusis (LASIK), photorefractive keratectomy (PRK), small intrastromal lenticule extraction (SMILE) are commonly used to correct myopia, astigmatism, hyperopia and presbyopia as well. The change in curvature is obtained in all cases by the subtraction of stroma in order to modify the corneal dioptric power. However, these changes in curvature do produce alterations in the corneal epithelium that, most interestingly, may induce modifications in the refraction as well. The way in which epithelial changes occur may vary due to several factors such as the type of correction performed, the diameter, the amount of tissue subtraction, or the corneal asphericity.
This chapter describes the epithelial changes by means of the MS-39 epithelial map by comparison with other curvature and elevation maps from the same instrument. Thus, providing us some clarification for personal interpretation of changes that are not commonly found. Except for the first one, all photos are presented in the same way as shown in the maps below (Figure 1).

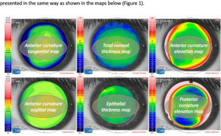

Figure 1. *Epithelial maps: different measurements.*

1. NORMAL FEATURES AFTER LASER REFRACTIVE SURGERY

Usually in normal, pre-surgical eyes, the corneal epithelium has a variable thickness ranging from 40 to 60 microns with no significant differences between the center and the periphery (Figure 2).
When correcting myopic refractive errors, a thicker in-the-center lenticule of stromal tissue is removed.

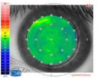

Figure 2. *Epithelial thickness.*

Usually this causes a counterbalancing response from the corneal epithelium which becomes thicker in the center in comparison to the periphery. This central epithelium thickening occurs with other modifications. Higher myopic corrections, thicker lenticule removal and smaller lenticule diameters are associated with higher central epithelial thickening.
The maps below show a relatively low myopic correction performed with a large ablation zone. Note the bottom-central image (epithelium) relatively thicker only in the center than the periphery (Figures 3, 4).

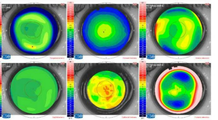

Figure 3. *Low myopic correction: epithelial changes.*

This second set of maps show a higher myopic correction performed with a smaller ablation zone. Note the thicker epithelium (Figure 4).

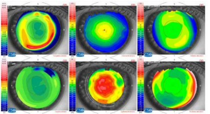

***Figure 4.** High myopic correction: epithelial changes.*

The following two sets of maps show the epithelial changes after hyperopic refractive surgery. Here again, the epithelium tends to compensate for the induced change in curvature by becoming thinner in the center than in the periphery. The correlated modifications are the same. This first set shows the pattern of a small correction performed with a wider ablation zone (Figure 5).

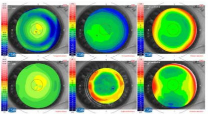

***Figure 5.** Low hyperopic correction: epithelial changes.*

The following maps (Figure 6) instead, show the epithelial changes after a higher hyperopic correction performed with a smaller ablation zone. These epithelial changes may have some impact on the results of laser refractive surgery. A thicker epithelium in the center of the cornea relative to the periphery may induce a myopic shift. Conversely, a thinner epithelium in the center of the cornea relative to the periphery may induce a hyperopic shift. An enhancement procedure involving epithelial removal may raise the question whether the cornea would re-epithelialize, leading to further unpredictable outcomes.

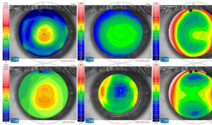

Figure 6. Hyperopic correction.

2. ATYPICAL EPITHELIAL THICKNESS CHANGES

Anomalies in the thickness of the epithelial layer may lead to a misinterpretation of the clinical picture after laser refractive surgery. The following maps show the case of what appears to be a decentration after myopic LASIK in corneal topography. All maps, curvatures and heights as well as the corneal thickness map, show the flattened area to be decentered inferior-nasally. Only with the aid of the epithelial map, is it possible to appreciate that the relative steepening of the superior-temporal area is related to the uneven epithelial thickness, and not or only in part to a decentered ablation (Figure 7).

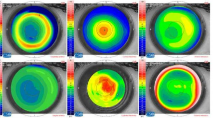

***Figure 7.** Myopic LASIK with uneven epithelial changes. The post-op anterior maps looks like a decentered treatment due to the asymmetric epithelial healing.*

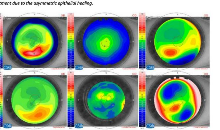

***Figure 8.** Myopic LASIK correction: uneven epithelial thickness.*

The most striking changes in epithelial thickness uniformity occur when the posterior curvature tends to bulge and develop into a corneal ectasia. As in keratoconus, in which the anterior corneal curvature steepens and the epithelium remodels by smoothening the change in curvature to become thinner at the apex, also in refractive surgery-induced corneal ectasia, the same modification occurs. As the next maps demonstrate, the epithelium becomes thinner where the steepening and bulging occurs (Figure 8).

In Figures 9 and 10, two cases are shown where the correlation between the thinner epithelial areas, the steepening and bulging is quite evident.

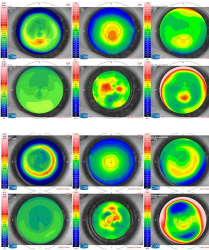

Figures 9-10. *Epithelial changes after bulging*

Most interestingly, notice that the epithelial changes in thickness to smooth out the corneal irregularity may occur *before* a change in curvature of the anterior surface has been detected. The following maps show the case of a very mild posterior curvature bulging, in which the epithelium remodels itself to conceal the ectasia when observing the anterior corneal curvature or the anterior surface elevation map (Figure 11).

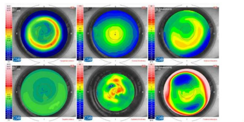

Figure 11. Mild posterior bulging with epithelial remodeling.

TAKE HOME MESSAGE

Timely measurement of the corneal epithelial thickness after laser refractive surgery helps the refractive surgeon to gain a better understanding of possible clinical and refractive outcomes. It contributes to evaluate difficult cases that otherwise cannot be understood without this exciting technology. The corneal epithelial map is an invaluable tool for diagnosing varied conditions and making interventional and therapeutic decisions.

REFERENCES

1. *Role of the corneal epithelium measurements in keratorefractive surgery. Salomão MQ, Hofling-Lima AL, Lopes BT, Canedo ALC, Dawson DG, Carneiro-Freitas R, Ambrósio R Jr. Curr Opin Ophthalmol. 2017 Jul;28(4):326-336. doi: 10.1097/ICU.0000000000000379. Review.*
2. *Corneal epithelial thickness mapping using Fourier-domain optical coherence tomography for detection of form fruste keratoconus. Temstet C, Sandali O, Bouheraoua N, Hamiche T, Galan A, El Sanharawi M, Basli E, Laroche L, Borderie V. J Cataract Refract Surg. 2015 Apr;41(4):812-20. doi: 10.1016/j.jcrs.2014.06.043.*
3. *In Vivo 3-dimensional corneal epithelial thickness mapping as an indicator of dry eye: preliminary clinical assessment. El Sanharawi M, Sandali O, Borderie V, Laroche L. Am J Ophthalmol. 2014 May; 157(5):1116. doi: 10.1016/j.ajo.2014.01.029. No abstract available.*
4. *Longitudinal postoperative lasik epithelial thickness profile changes in correlation with degree of myopia correction. Kanellopoulos AJ, Asimellis G. J Refract Surg. 2014 Mar;30(3):166-71. doi: 10.3928/1081597X-20140219-01.*
5. *Refractive and topographic errors in topography-guided ablation produced by epithelial compensation predicted by 3D Artemis VHF digital ultrasound stromal and epithelial thickness mapping. Reinstein DZ, Archer TJ, Gobbe M. J Refract Surg. 2012 Sep;28(9):657-63. doi: 10.3928/1081597X-20120815-02.*
6. *Thickness mapping of the cornea and epithelium using optical coherence tomography. Haque S, Jones L, Simpson T. Optom Vis Sci. 2008 Oct;85(10):E963-76. doi: 10.1097/OPX.0b013e318188892c.*

17

CORNEAL ULCERS

ACUTE MANIFESTATION AND CORNEAL HEALING

DOMENICO SCHIANO LOMORIELLO, M.D.
IRCCS Fondazione G.B. Bietti - Rome, Italy

A corneal ulcer is one of the main causes for visual impairment that occasionally leads to the need for a corneal transplant or for phototherapeutic keratectomy. Currently corneal OCT has demonstrated to be a useful tool for the clinical approach to inflammatory and infective ulcers. The AS-OCT can directly visualize, measure and monitor in vivo parameters of corneal inflammatory disease.
The MS-39 presents the highest image resolution among all commercially available AS-OCT instruments, and further offers the possibility of measuring the pachymetric map along with the anterior and posterior curvature maps. The set of all the acquired images allows the clinician to evaluate in a more complete way the optical alterations due to an ulcer and its impact on visual quality.

1. CORNEAL ULCER WITH ANTERIOR CHAMBER INVOLVEMENT

Corneal ulcers in the acute phase are clearly visible with the AS-OCT as an area of stromal hyperreflectivity associated with thinning. The corneal epithelium is not often clearly visible. When the presence of a corneal ulcer also causes an anterior chamber reaction, we can observe a slight and not well-defined aqueous hyperreflectivity due to the inflammatory infiltration. In Figure 1 we can see an ulcer, negative for culture scraping for bacteria, fungus and acanthamoeba, with a PCR that resulted positive for HSV type 1.

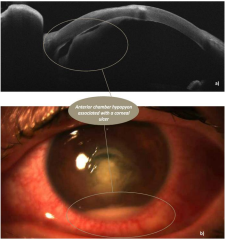

Figure 1 a-b. AS-OCT and clinical image.

Figure 2 shows the same patient after the healing of the ulcer. The hypopyon is completely reabsorbed and the anterior chamber appears empty. The corneal scar from the ulcer is easily visible as a hyperreflective subepithelial area in the OCT image. Central corneal thickness returned to within normal values but the anterior tangential curvature map demonstrates a central flattening surrounded by an increase of round shaped curvature (Figures 3).

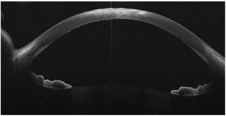

Figure 2. Resolution of the corneal ulcer of Figure 1.

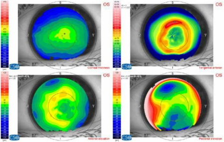

Figure 3. Topographic maps after the healing of the ulcer.

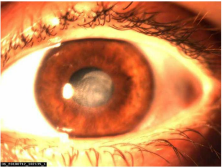

Figure 4. *Frontal slit lamp image after the healing of the ulcer.*

2. PERIPHERAL CORNEAL ULCER

Peripheral corneal ulcers with AS-OCT often appear as thinning areas associated with an increase of reflectivity (Figure 5a). The topography shows an alteration of the peripheral corneal curvature with an increase of corneal aberrations and irregularity (Figure 5b). These types of ulcers can often be secondary to staphylococcus.

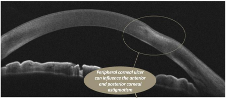

Figure 5a. *AS-OCT sectional image of a peripheral corneal ulcer.*

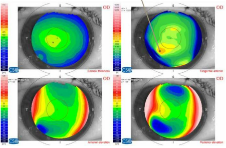

Figure 5b. *Topographic maps.*

3. CORNEAL OPACITY

After a corneal ulcer is healed, we can often observe an intrastromal hyperreflectivity of variable depth (Figure 6a). The epithelium is clearly visible as a separate layer. Corneal thickness is normal but there is an increase in the anterior curvature in the area surrounding the scar (Figure 6b).

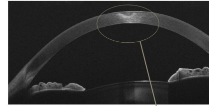

Figure 6a. Central corneal opacity secondary to a bacterial ulcer.

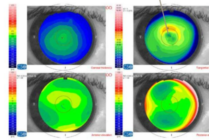

Figure 6b. Corneal scar topographical images.

4. CORNEAL ULCER WITH DALK

Sometimes corneal ulcers can affect patients who previously underwent a corneal transplant. The follow up with AS-OCT shows the depth of the ulcer and the condition of the stromal recipient bed. In this image (Figure 7) you can see a patient operated with a Descemetic DALK utilizing the big-bubble technique and presenting a severe corneal peripheral ulcer due to an HSV infection in the donor cornea. The pachymetric map shows the corneal thinning in the area of the ulcer, while the anterior and posterior altimetric and tangential maps highlighted paracentral bulging (Figure 8).

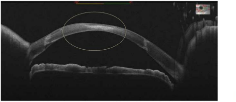

Figure 7. *HSV corneal ulcer in DALK patient. The corneal infiltration does not reach the donor-host interface.*

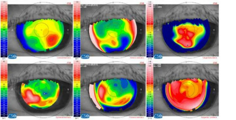

Figure 8. *Corneal paracentral bulging: topographic aspects.*

5. CORNEAL ULCER WITH DSAEK

When corneal ulcers affect a patient who previously underwent corneal endothelial surgery, there is the risk of damage to the implanted tissue. The follow up with AS-OCT allows the clinician to monitor the depth of the ulcer extension and thus the integrity of the deepest layer of the donor tissue (Figure 9).

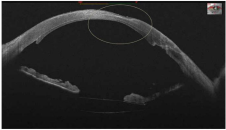

Figure 9. *A central corneal ulcer in the stromal-host tissue of a patient who underwent corneal endothelial surgery.*

TAKE HOME MESSAGE

High resolution AS-OCT, such as the MS-39, is a fundamental tool in clinical practice for cases of corneal ulcer and corneal infiltration. The AS-OCT images allows the clinician to achieve a more complete understanding not only of the true extension and morphological features of the inflammatory process, but also aids in arriving at an etiological diagnosis. Furthermore, the integration of OCT images with the pachymetric (OCT based) map and the anterior and posterior topographic maps is a very useful tool in the management of these patients. In fact, it permits a better understanding of the visual impairment caused by the ulcerative process thus improving the outcome of clinical and surgical interventions.

REFERENCES

1. *Konstantopoulos A, Kuo J, Anderson D et al. Assessment of the use of anterior segment optical coherence tomography in microbial keratitis. Am J Ophthalmol. 2008 Oct; 146(4):534-542.*
2. *Konstantopoulos A, Yadegarfar G, Fievez M, Anderson DF, Hossain P. In vivo quantification of bacterial keratitis with optical coherence tomography. Invest Ophthalmol Vis Sci. 2011 Feb 25; 52(2):1093-7*
3. *Yenerel NM, Kucumen RB, Gorgun E. The complementary benefit of anterior segment optical coherence tomography in penetrating keratoplasty. Clin Ophthalmol. 2013; 7:1515-23.*
4. *Takezawa Y, Suzuki T, Shiraishi A. Observation of Retrocorneal Plaques in Patients With Infectious Keratitis Using Anterior Segment Optical Coherence Tomography. Cornea. 2017 Oct; 36(10): 1237-1242.*

CORNEAL MORPHOLOGY IN ADVANCED KERATOCONUS

EPITHELIAL STROMAL INTERACTIONS AND CORNEAL RESHAPING

LEONARDO MASTROPASQUA, M.D. - MARIO NUBILE, M.D.
National High Tech Eye Center, University "G. D'Annunzio" - Chieti and Pescara, Italy

Advanced keratoconus can be often associated with anterior stromal opacities, needing to be clinically interpreted to ensure a correct surgical management when intervention is indicated. Central stromal scarring may be of different origin and morphology in severe keratoconus. Slit lamp examination and anterior surface topography are not always complete for determining the structural changes in such cases.

1. ADVANCED CENTRAL KERATOCONUS WITH STROMAL SCARRING

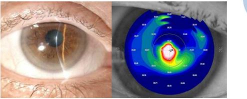

Figure 1. Slit lamp image and topographic representation of a central keratoconus.

In this Figure 1, an advanced keratoconus with a central stromal scar is presented. On the left side the slit lamp picture is shown. On the right side the tangential topographic map of the anterior corneal surface shows the central "nipple-shaped" hyperprolate area corresponding to the cone and to the scarred stroma.

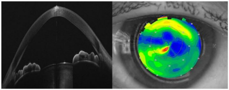

***Figure 2.** Advanced KC.*

In such a case of advanced keratoconus, with central stromal scarring, the high resolution anterior segment OCT and corneal epithelial map are shown: in Figure 2, on the left the anterior segment OCT shows a dense stromal hyperplastic leucoma with anterior corneal surface bulging. On the right, the epithelial map indicates the marked epithelial irregularities and thinning over the cone and over the scarred areas.

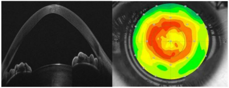

***Figure 3.** Advanced KC after CXL and PTK.*

In Figure 3, after corneal cross-linking (CXL) followed by excimer laser PTK of the central stromal scar, on the left the anterior segment OCT section is shown. The image highligths the anterior stromal profile inversion, with recovery of stromal transparency. On the right, the epithelial map illustrates the epithelial thickening and regularization.

2. ADVANCED KERATOCONUS WITH DIFFUSE CENTRAL STROMAL SCAR

In the majority of cases the occurrence of anterior stromal opacification in keratoconus does not significantly alter neither the stromal profile nor the epithelial distribution over the opaque area. Generally, the anterior corneal curvature is partially affected by these morphological changes.

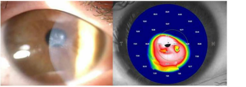

***Figure 4.** Advanced KC.*

In Figure 4 an advanced keratoconus case with a central stromal scar and Bowman's membrane rupture is presented. On the left the slit lamp picture is shown. On the right the tangential map of the anterior corneal surface shows an evident ectatic area with extremely high curvature in the cone region.

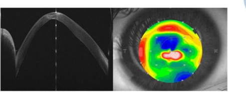

***Figure 5.** Advanced KC: AS-OCT section and epithelial map.*

In Figure 5, on the left, the anterior segment OCT shows an evident stromal depression with anterior stromal curvature thinning and inversion. The hyperprolaticity of the anterior surface is due to the extremely marked epithelial thickening that occurs over the depressed stromal area, as shown in the image on the right (epithelial map). In this case only DALK would be indicated. The AS-OCT analysis of an epithelial map profile (Figure 5 - right side), correlated with topography clearly indicates that the anterior corneal curvature is maintained by epithelial hyperplasia that occurs over the stromal depressed scarred zone.

3. CORNEAL RE-SHAPING IN ADVANCED KERATOCONUS WITH STROMAL LENTICULE ADDITION KERATOPLASTY

As an alternative to deep anterior lamellar (DALK) or penetrating keratoplasty (PK), the possibility of using intrastromal tissue implantation has been proposed.
Particularly, the stromal lenticule addition keratoplasty procedure has been shown to be clinically efficient in patients with central keratoconus, by improving the corneal shape, increasing visual acuity and reducing astigmatism. Negative meniscus-shaped lenticule addition can induce flattening of the cone along with increasing corneal thickness (Figure 6).

Figure 6. *Advanced central keratoconus with a transparent central cornea. Left: slit lamp image. Right: high resolution anterior segment OCT.*

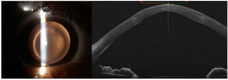

Figure 7. *KC after SLAK.*

The same case of the previous image after SLAK procedure, performed using femtosecond laser technology. Left: slit lamp photo with transillumination in a dilated pupil illustrates the intrastromal lenticule profile (Figure 7).
High resolution anterior segment OCT in the same case shows the negative meniscus profile of the lenticule integrated into the recipient stroma, hence reshaping the corneal morphology in the ectatic zone.

TAKE HOME MESSAGE

A high resolution AS-OCT, such as the MS-39, is a useful tool for understanding the relationship between the anterior corneal curvature, stromal morphology and thickness, and finally epithelial hyperplasia in advanced keratoconus. Clinical management with a particular emphasis on surgical decisions can be facilitated by a more complete comprehension in such cases of the true anterior corneal morphology.

REFERENCES

1. *Schallhorn JM, Tang M, Li Y, Louie DJ, Chamberlain W, Huang D. Distinguishing between contact lens warpage and ectasia: Usefulness of optical coherence tomography epithelial thickness mapping. J Cataract Refract Surg. 2017 Jan; 43(1):60-66.*
2. *Mastropasqua L, Nubile M. Corneal thickening and central flattening induced by femtosecond laser hyperopic-shaped intrastromal lenticule implantation. Int Ophthalmol. 2017 Aug; 37(4):893-904.*
3. *Mastropasqua L, Nubile M, Salgari N, Mastropasqua R. Femtosecond Laser-Assisted Stromal Lenticule Addition Keratoplasty for the Treatment of Advanced Keratoconus: A Preliminary Study. J Refract Surg. 2018 Jan 1;34(1):36-44.*

19

THE MANAGEMENT OF GRAFT DETACHMENT AFTER DESCEMET MEMBRANE ENDOTHELIAL KERATOPLASTY (DMEK)

GIOVANNI ALESSIO, M.D. - MARIA GABRIELLA LA TEGOLA, M.D. - ROBERTA DIMA, PhD, Science, Neuro-Science and Sensory Organs- Department of Ophthalmology, University of Bari Bari, Italy

Descemet's stripping automated endothelial keratoplasty (DSAEK) and Descemet's membrane endothelial keratoplasty (DMEK) are both considered procedures of choice for the treatment of corneal endothelial failure due to Fuchs' dystrophy or bullous keratopathy. Although visual results after DMEK seem to be superior to those after DSAEK, donor graft detachment or dislocation are more common after DMEK.
We present a case of DMEK performed for Fuchs' dystrophy, complicated with graft detachment that subsequently needed DSAEK. In this case, the MS-39 OCT images were very useful to detect the donor graft position and its adherence to the host stroma during the postoperative period.

ONE DAY AFTER DMEK

One day after DMEK, the donor graft was difficult to identify, but the MS-39 OCT revealed a limited detachment in the central cornea (Figure 1). The anterior chamber was deep due to the presence of a big air bubble.

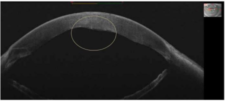

Figure 1. *Limited central graft detachment one day after DMEK.*

THREE DAYS AFTER DMEK

Three days after DMEK, diffuse corneal edema was present. The graft was not visible by slit lamp examination (Figure 2).

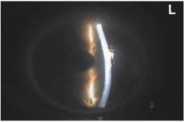

Figure 2. Diffuse corneal edema at the slit lamp.

The OCT images revealed a complete detachment of the graft that appeared to be curled into the anterior chamber. Corneal edema and bullous keratopaty were also visible (Figure 3).

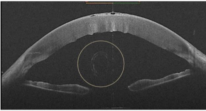

Figure 3. Curled detached graft in the anterior chamber.

Repositioning of the graft and a new injection of air into the anterior chamber were performed (Figure 4).

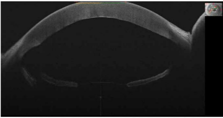

Figure 4. *Completely adherent graft after repositioning and air injection into the anterior chamber.*

ONE DAY AFTER RE-BUBBLING

One day after rebubbling, edema, a large detachment, and dislocation of the graft were recognized by the MS-39 OCT. An air bubble was still present in the anterior chamber (Figure 5).

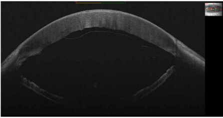

Figure 5. *Dislocation and detachment of the graft one day after graft repositioning and re-bubbling.*

Two days after the reintervention, OCT images revealed a complete dislocation of the graft, that appeared crumpled and adherent to the stroma only in a few areas (Figure 6).

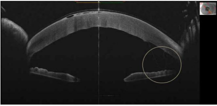

Figure 6. *Dislocated and crumpled graft at the inferior part of the anterior chamber.*

DSAEK AFTER DMEK

Since the two reinterventions proved to be ineffective, DSAEK was carried out after removing the detached DMEK graft. The complete restoration of corneal transparency was achieved (Figure 7).

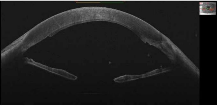

Figure 7. *Successfully DSAEK and edema resolution.*

TAKE HOME MESSAGE

The MS-39 OCT was essential during the follow-ups to visualize the graft. The correct diagnosis is mandatory for appropriate surgical planning.

REFERENCES

1. *Stuart AJ, Romano V, Virgili G, Shortt AJ. Descemet's membrane endothelial keratoplasty (DMEK) versus Descemet's stripping automated endothelial keratoplasty (DSAEK) for corneal endothelial failure. Cochrane Database Syst Rev 2018 Jun 25;6 CD012097*

20

CORNEAL LATTICE DYSTROPHY

GIOVANNI ALESSIO, M.D. - MARIA GABRIELLA LA TEGOLA, M.D. - MARCO TRENTADUE, M.D.
Department of Basic Medical Science, Neuro-Science and Sensory Organs
Department of Ophthalmology, University of Bari- Bari, Italy

Lattice dystrophy is an inherited corneal disorder described as a localized corneal amyloidosis. Early clinical features include subepithelial opacities, white dots in the anterior stroma and refractile lines easily visible by retroillumination at the slit lamp. In the more advanced stages, the lines can reach into the deep stroma and may opacify with stromal haze occurring, causing severe visual loss. The peripheral cornea and the endothelium are not involved (Figure 1).
Depending on the localization and extension of the opacities, treatments for lattice dystrophy include excimer laser ablation, superficial anterior lamellar keratoplasty (SALK), deep anterior lamellar keratoplasty (DALK), or penetrating keratoplasty (PK). Therefore, it is important to measure the depth of the opacities in order to choose the appropriate treatment, and also to be cognizant of the precise corneal pachymetry to plan the surgery.

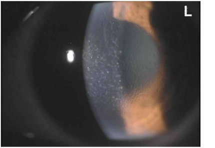

Figure 1. *Slit lamp image of corneal lattice dystrophy.*

The Scheimpflug images may be ambiguous in detecting the exact position of the scars (Figure 2a), due to light scattering, and may generate an incorrect pachymetric map 3 (Figure 2b). The MS-39 OCT, instead, provides an exact identification and localization of the opacities (Figure 3a), as well as a precise pachymetric map (Figure 3b).

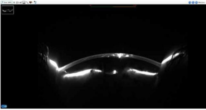

Figure 2a. Scheimpflug image of corneal lattice dystrophy.

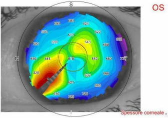

Figure 2b. Pachymetric map obtained by means of a Scheimpflug-based corneal topographer.

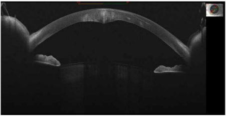

Figure 3a. *MS-39 OCT image of corneal lattice dystrophy. Opacities are well identified and can be measured. Central corneal thickening, due to severe scarring is easily recognized.*

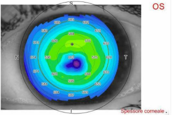

Figure 3b. *Pachymetric map obtained with the MS-39.*

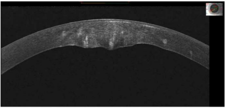

Figure 4. High-resolution MS-39 OCT image of lattice dystrophy involving the central corneal stroma. Deformation of endothelial profile due to the deep scarring can be noted.

In this case, the opacities reach the deep stroma near to the endothelium, making the separation between the deep stroma and the Descemet's membrane difficult to envision during DALK (Figure 4).

TAKE HOME MESSAGE

The visualization of corneal opacities is necessary in order to decide the appropriate surgical treatment. An exact pachymetric map aids in the surgical planning during DALK, so as to avoid perforation while trephining.

REFERENCES

1. *Arora R. Deep anterior lamellar keratoplasty or penetrating keratoplasty in lattice corneal dystrophy. Indian J Ophthalmol. 2018 May;66(5):673-674*

21

ORTHOKERATOLOGY

ANTONIO CALOSSI, O.D.
University of Florence- Certaldo, Italy

Orthokeratology is a non-surgical technique which allows to reduce, vary or eliminate a refractive error through the programmed application of contact lenses specifically designed to modify the corneal profile in a controlled manner.[1-2] Lenses produce a temporary reduction of the refractive error by changing the shape of the cornea. This is made possible thanks to the plasticity of corneal tissue, especially at the epithelial level.[3] The re-shaping of the cornea modifies the ocular refractive power and, if the remodeling is adequately controlled, it is possible to vary the corneal power in a precise way, thus producing a compensation of the refractive error. In the case of myopia, orthokeratology induces a central flattening with an increase peripheral curvature. In regard to the correction of hypermetropia, the opposite occurs producing a central curvature steepening with a concurrent flattening in the mid-periphery. In modern over-night orthokeratology, the lenses are worn only during sleep and then removed immediately after awakening. This results in a good quality of vision during the day, with no need for glasses or contact lenses.[4, 5]

Orthokeratology is generally recommended for low to moderate myopic patients (up to 6 diopters), in case of hypermetropia (up to 3 diopters) and in some cases of astigmatism.[6-8] Furthermore, this technique can also be of benefit in some selected cases of presbyopia.[9] In addition to the refractive correction effects, orthokeratology can effectively slow down myopia progression and eyeball elongation in younger patients.[10]

Since its beginning orthokeratology has undergone significant changes, involving new geometries, design, and materials. Newer lenses are safer to apply, have high oxygen permeability and are more comfortable to wear while sleeping or keeping the eyes closed.[13-15] Furthermore, recent advanced diagnostic tools allow a deeper understanding of orthokeratology and a more precise monitoring of patients during all the treatment phases. An anterior segment OCT, such as the CSO MS-39, represents one of the last innovations in this field.

Since nothing is surgically removed, orthokeratology does not induce any volumetric change in the cornea, as it occurs with photoablative surgical techniques. Therefore, in order to obtain this type of curvature change, which is correlated to the reduction of refractive error, it is necessary to shape the corneal tissue. Current available technologies allow us to better understand how alterations occur, the quantitative values and the modifications that might occur during the treatment phases.

Figure 1 shows a corneal section acquired by the OCT MS-39 of an eye on which an ESA lens is applied for myopic orthokeratology (Esavision Technology, Verona, Italy).[16-18] In this figure the peripheral support zone, the apical touch zone and the zone of maximum clearance in mid-periphery can be observed. This lens, worn with eyes closed, acts as a remodeler, shaping the underlying corneal tissue. The lens exerts a pressure in the peripheral contact zone moving the tissue towards the maximum clearance zone of the lens. Thus, we obtain peripheral flattening which induces a mid-periphery curvature, with consequential secondary flattening of the central zone (Figure 2). A slight central pressure can further increase the flattening of the corneal optic zone.

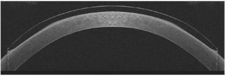

Figure 1. Corneal section acquired by OCT, of an eye on which an ESA lens is applied for the myopia compensation. We note the peripheral support zone, the apical touch zone and an area of maximum clearance on the mid-periphery.

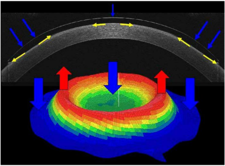

Figure 2. The lens exerts a pressure in the peripheral contact zone moving the tissue towards the maximum clearance zone of the lens. Therefore, we obtain a peripheral flattening which induces a mid-peripheral curvature, with consequential secondary flattening of the central zone.

The epithelium is the softest and the most malleable section of the cornea, therefore it is reasonable to think that modeling takes place on the epithelial level. This has been confirmed by two histological studies on animal models. The first was conducted by Matsubara et al. on rabbit eyes.[21] In this work, the thickness of the corneal epithelium showed a topographic variation consistent with the orthokeratological effect we described above, while the results of the histochemical study showed no significant changes in epithelial function, and absence of metabolic changes induced by the compression forces of the lens. A second work was conducted by Jennifer Choo et al. on cats.[22] This study demonstrated that cell compression occurs within the first hours and a redistribution of epithelial cells occurs due to the remodeling action of the lens. This might explain the stable refractive results of an effective orthokeratology treatment.

Anterior segment OCT with the MS-39 provides not only a complete corneal topography and tomography, but also an accurate analysis of the epithelial thickness in vivo.

Figures 3 and 4 show the horizontal scan of the cornea of a patient undergoing orthokeratology for myopia, in this case for a correction of -4.50 D. The tomographic section acquired with the AS-OCT MS 39 shows a differentiated corneal epithelial thickness distribution, with a symmetrical thinning in the periphery of the cornea and a relative thickening in the mid-periphery.

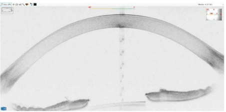

Figure 3. *The horizontal section of the anterior segment performed with the AS-OCT MS39 shows a differentiated corneal epithelial thickness distribution, with symmetrical thinning of the corneal peripheral area (A) and a relative thickening in mid-periphery (B).*

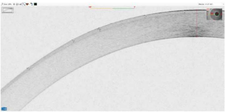

Figure 4. *Magnification of Figure 3 shows the mid-peripheral thickening of the cornea.*

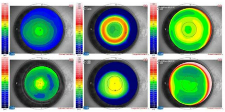

Figure 5. *Topographic summary of the measurements performed with the AS-OCT MS-39.*

Figure 5 shows a topographic summary of measurements performed with the AS-OCT MS 39. In sequence, from top to bottom and from left to right: the pachymetric map of the entire cornea and of the corneal epithelium; the curvature of the anterior and posterior surfaces; the anterior and posterior elevation. Data show that shape variations are all relative to the anterior surface of the cornea, with an increase in relative elevation in the paracentral cornea that corresponds to a region of relative thickening of the epithelium, and an increase in curvature, as evidenced by the concentric red ring in the pupil. We can also observe a slight central thinning of the epithelium and a flattening of the curvature that produces the compensation of the refractive error, as well as a concentric flattening zone in the peripheral region, corresponding to the contact lens alignment zone, and a reduction of corneal surface elevation, due to the compression exerted by the lens. Figure 6 shows the numerical values of the effects induced by corneal modeling.

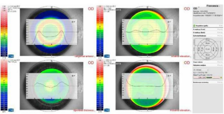

Figure 6. *Profiles of anterior curvature, corneal thickness, anterior and posterior elevation.*

In Figure 7 the refractive effects of corneal modeling can be analyzed. Corneal modeling produced by the orthokeratology lens was obtained by epithelial thicknesses redistribution, consequently inducing an altimetric variation of the corneal surface. This controlled variation of the curvature of the anterior surface of the cornea results in a precise and regular reduction of the dioptric power of the central cornea.

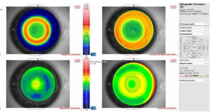

Figure 7. *Topographic summary utilizing a corneal refractive power map, anterior curvature, anterior elevation and epithelial pachymetry.*

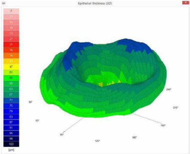

Figure 8. *3D representation of epithelial thickness measured with the AS-OCT MS-39.*

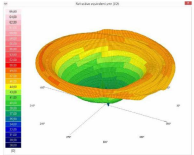

Figure 9. *3D representation of the refractive power of the cornea calculated by ray-tracing from the AS-OCT MS-39 software.*

The three-dimensional representation of the epithelial map shown in Figure 8 clearly demonstrates the modeling effect induced by the contact lens. This provided a redistribution of the corneal refractive power, with a concurrent reduction of dioptric power within the optical zone, as shown in Figure 9.

TAKE HOME MESSAGE

In clinical practice, in addition to standard refractive and biomicroscopic examination, corneal topography is the instrumental of choice to verify the successful outcome of orthokeratology. The mechanisms that govern corneal modeling through orthokeratology are still far from complete understanding.[3,19,23-33] High-definition tomographic analysis performed with the AS-OCT MS39 allows the clinician to measure the effects of orthokeratology on various structures of the cornea, in particular the epithelium, and a better comprehension of the mechanism of action for this technique.

REFERENCES

1. *Jessen GN. Orthofocus techniques. Contacto 1962;6:200-204.*
2. *Grant SC, May CH. Orthokeratology - a therapeutic approach to contact lens proceduress. Contacto 1970;14:3-16.*
3. *Reinstein DZ, Gobbe M, Archer TJ, Couch D, Bloom B. Epithelial, stromal, and corneal pachymetry changes during orthokeratology. Optom Vis Sci 2009;86:E1006-1014.*
4. *Nichols JJ, Marsich MM, Nguyen M, Barr JT, Bullimore MA. Overnight orthokeratology. Optom Vis Sci 2000;77:252-259.*
5. *Barr JT, Rah MJ, Jackson JM, Jones LA. Orthokeratology and corneal refractive therapy: a review and recent findings. Eye Contact Lens 2003;29:S49-53; discussion S57-49, S192-194.*
6. *Swarbrick HA. Orthokeratology review and update. Clin Exp Optom 2006;89:124-143.*
7. *Paune J, Cardona G, Quevedo L. Toric double tear reservoir contact lens in orthokeratology for astigmatism. Eye Contact Lens 2012;38:245-251.*
8. *Calossi A. Mixed astigmatism treated with a dual-toric ortho-k design. Contact Lens Spectrum 2013;28:49-50.*
9. *Calossi A. Orthokeratology and presbyopia. Cataract & Refractive Surgery Today Europe 2010;April:71-76.*
10. *Wen D, Huang J, Chen H, et al. Efficacy and Acceptability of Orthokeratology for Slowing Myopic Progression in Children: A Systematic Review and Meta-Analysis. J Ophthalmol 2015;2015:360806.*
11. *Soni PS, Nguyen TT, Group XOOOS. Overnight orthokeratology experience with XO material. Eye Contact Lens 2006;32:39-45.*
12. *Lipson MJ. Long-term clinical outcomes for overnight corneal reshaping in children and adults. Eye & Contact Lens 2008;34:94-99.*
13. *Zhong X, Chen X, Xie RZ, et al. Differences between overnight and long-term wear of orthokeratology contact lenses in corneal contour, thickness, and cell density. Cornea 2009;28:271-279.*
14. *Lum E, Swarbrick HA. Lens Dk/t influences the clinical response in overnight orthokeratology. Optom Vis Sci 2011;88:469-475.*
15. *Liu YM, Xie P. The Safety of Orthokeratology--A Systematic Review. Eye Contact Lens 2016;42:35-42.*
16. *Calossi A. Metodo di personalizzazione di una lente per il trattamento della miopia. Patent number: BO2002A000595. Italy; 2002.*
17. *Calossi A. A new customized esa-curve reverse geometry lens design for overnight orthokeratology. 33° European Contact Lens Society of Ophthalmologists Congress. Venezia; 2003.*
18. *Calossi A. Efficacy and safety of overnight orthokeratology by means of a customized ESA Curve reverse geometry lens. 2nd annual Global Orthokeratology Symposium. Toronto; 2004.*
19. *Haque S, Fonn D, Simpson T, Jones L. Corneal and epithelial thickness changes after 4 weeks of overnight corneal refractive therapy lens wear, measured with optical coherence tomography. Eye Contact Lens 2004;30:189-193; discussion 205-186.*
20. *Qian Y, Xue F, Huang J, Qu X, Zhou X, Lanen-Wanek DV. Pachymetry map of corneal epithelium in children wearing orthokeratology contact lenses. Curr Eye Res 2014;39:263-270.*
21. *Matsubara M, Kamei Y, Takeda S, Mukai K, Ishii Y, Ito S. Histologic and histochemical changes in rabbit cornea produced by an orthokeratology lens. Eye Contact Lens 2004;30:198-204; discussion 205-196.*
22. *Choo JD, Caroline PJ, Harlin DD, Papas EB, Holden BA. Morphologic changes in cat epithelium following continuous wear of orthokeratology lenses: a pilot study. Cont Lens Anterior Eye 2008;31:29-37.*
23. *Polse KA, Brand RJ, Vastine DW, Schwalbe JS. Corneal change accompanying orthokeratology. Plastic or elastic? Results of a randomized controlled clinical trial. Arch Ophthalmol 1983;101:1873-1878.*
24. *Alharbi A, Swarbrick HA. The effects of overnight orthokeratology lens wear on corneal thickness. Invest Ophthalmol Vis Sci 2003;44:2518-2523.*
25. *Owens H, Garner LF, Craig JP, Gamble G. Posterior corneal changes with orthokeratology. Optom Vis Sci 2004;81:421-426.*
26. *Cheah PS, Norhani M, Bariah MA, Myint M, Lye MS, Azian AL. Histomorphometric profile of the corneal response to short-term reverse-geometry orthokeratology lens wear in primate corneas: a pilot study. Cornea 2008;27:461-470.*
27. *Tsukiyama J, Miyamoto Y, Higaki S, Fukuda M, Shimomura Y. Changes in the anterior and posterior radii of the corneal curvature and anterior chamber depth by orthokeratology. Eye Contact Lens 2008;34:17-20.*
28. *Gifford P, Au V, Hon B, Siu A, Xu P, Swarbrick HA. Mechanism for corneal reshaping in hyperopic orthokeratology. Optom Vis Sci 2009;86:e306-311.*
29. *Chan B, Cho P, Mountford J. Relationship between corneal topographical changes and subjective myopic reduction in overnight orthokeratology: a retrospective study. Clin Exp Optom 2010;93:237-242.*
30. *Nieto-Bona A, Gonzalez-Mesa A, Nieto-Bona MP, Villa-Collar C, Lorente-Velazquez A. Long-term changes in corneal morphology induced by overnight orthokeratology. Curr Eye Res 2011;36:895-904.*
31. *Yoon JH, Swarbrick HA. Posterior corneal shape changes in myopic overnight orthokeratology. Optom Vis Sci 2013;90:196-204.*
32. *Gonzalez-Mesa A, Villa-Collar C, Lorente-Velazquez A, Nieto-Bona A. Anterior segment changes produced in response to long-term overnight orthokeratology. Curr Eye Res 2013;38:862-870.*
33. *Li F, Jiang ZX, Hao P, Li X. A Meta-analysis of Central Corneal Thickness Changes With Overnight Orthokeratology. Eye Contact Lens 2016;42:141-146.*

22

POST-RK SCLERAL LENSES

RESTORING GOOD QUALITY OF VISION AFTER A LESS THAN OPTIMAL RADIAL KERATOTOMY OUTCOME

ANTONIO CALOSSI, O.D.
University of Florence - Certaldo, Italy

This case report describes a patient who underwent radial keratectomy (RK) 25 years ago. Twelve years later an enhancement was performed by PRK. Despite the initial successful outcome, the patient experienced progressive deterioration of visual quality, only partially improved with glasses. Night vision was severely compromised. Corneal RGP contact lenses gave poor results. Vision was within acceptable parameters with contact lenses, but the patient complained of low comfort level. In addition, lenses showed a tendency to decenter. The glasses in use were: OD -2.00 + 4.00 x 140, VA 5/10; OS -0.50 + 4.50 x 150, VA 5/10 and could not be improved upon.
Figures 1 and 2 show the incisions of the right eye radial keratotomy.

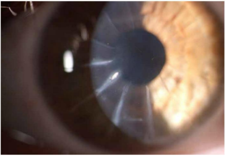

Figure 1. *The biomicroscopic examination shows the results of radial keratotomy.*

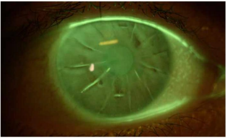

Figure 2. The biomicroscopic examination with fluorescein demonstrates even more evidently the results of the incisions.

Figures 3, 4 and 5 show the corneal sections obtained with the AS-OCT MS-39.

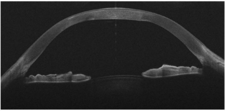

Figure 3. The horizontal meridian 0-180° scan notes a very oblate cornea, with an inhomogeneous thicknesses distribution.

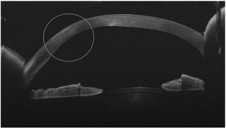

Figure 4. *The vertical meridian 90-270° scan notes a strong vertical asymmetry, with a protrusion in the lower part (on the left part of the image).*

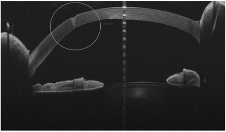

Figure 5. *In reference to the transverse incision, we note a not completely closed stromal incision, refilled with epithelium.*

Figure 6 shows a topographic summary obtained with the AS-OCT MS-39. Note the uneven corneal thickness distribution, a strong elevation asymmetry, a very prolate and asymmetrical shape of both the anterior and posterior face and a corneal refractive power with irregular and asymmetric distribution.

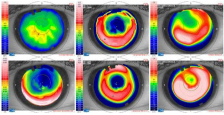

Figure 6. Topographic summary. From top to bottom and from left to right, note: the pachymetric map, the entire corneal refractive power distribution, the anterior and posterior curvature, the anterior and posterior surfaces and their altimetric dimensions.

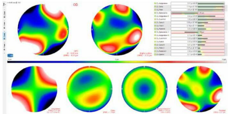

Figure 7. Corneal aberrometric summary obtained with the AS-OCT MS39.

Figure 7 shows the corneal aberrometric analysis. In addition to astigmatism, many high-order aberrations are present, and explain the visual symptoms reported by the patient, not entirely correctable with glasses. A rigid gas permeable contact lens was reapplied to obtain a regular optical surface. However, the oblate corneal shape, in addition to the notable asymmetry and the surface irregularity, did not allow to obtain a sufficient alignment with the corneal lenses. Specific inverse geometry designs gave poor results. Therefore, we decided to vault the cornea by application of a scleral lens. We applied an ICD 16.5 mini-scleral GP lens, customizing the parameters of the lens in order to obtain a good scleral support, in addition to an as homogeneous as possible corneal and limbal vault. The chosen Boston XO, Dk 100 lens material is very permeable to oxygen (Figure 8).

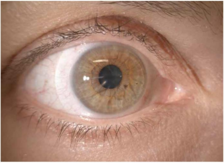

Figure 8. *Scleral lens.*

In the next image the high magnification shows the “no contact” between the scleral lens and the corneal surface (Figure 9).

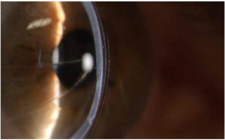

Figure 9. *The relationship between the lens and cornea, as can be noted with the slit lamp, shows the absence of contact between the lens and the cornea. Note the good clearance over the entire cornea.*

Figures 10 and 11 show the final lens after 8 hours from insertion. Appropriate corneal vaulting with a correct scleral alignment can be observed.

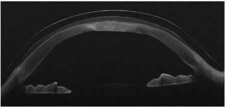

Figure 10. *The OCT scan grants a precise estimate of the applied lens: the clearance in the corneal area is optimal and the scleral alignment is uniform.*

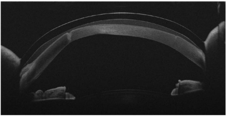

Figure 11. The OCT scan relative to the transverse incisions highlights the lack of contact at the most critical point of the cornea.

With the final lens, the patient obtained a visual acuity of 20/20 with good visual quality also in dim light conditions and night visio. Comfort was excellent and the daily wearing time was 12 hours. No adverse reactions were reported after one year.

TAKE HOME MESSAGE

This case demonstrates that patients who develop irregular corneal surfaces after refractive surgery and cannot be corrected with glasses, soft contact lenses or GP corneal lenses, may benefit from the use of modern scleral contact lenses. The high definition tomographic analysis performed by the AS-OCT MS-39 can effectively assist in the design and customization phase of lens fitting, in order to obtain the best possible lens alignment. AS-OCT can also monitor the effects of the lens over time.

NOTE

NOTE

NOTE

NOTE